이학석사학위논문

Feeding by the heterotrophic nanoflagellate *Katablepharis japonica* on red-tide organisms and interactions between the phototrophic dinoflagellate *Heterocapsa minima* and heterotrophic protists

종속영양성 미세편모류인 카타블레페리스 자포니카의 적조생물들 포식, 광합성 와편모류인 헤테로캡사 미니마와 종속영양성 원생생물의 상호작용 연구

2018 년 8 월

서울대학교 대학원

지구환경과학부 해양학전공

권 지 은

Abstract

Feeding by the heterotrophic nanoflagellate *Katablepharis japonica* on red-tide organisms and interactions between the phototrophic dinoflagellate *Heterocapsa minima* and heterotrophic protists

Ji Eun Kwon

School of Earth and Environmental Sciences
College of Natural Sciences
Seoul National University

Heterotrophic nanoflagellates are ubiquitous and known to be major predators of bacteria. However, the feeding of free-living heterotrophic nanoflagellates on phytoplankton is poorly understood, although these two components usually co-exist. To investigate the feeding and ecological roles of major heterotrophic nanoflagellates *Katablepharis* spp., the feeding ability of *Katablepharis japonica* on bacteria and

phytoplankton species and the type of the prey that *K. japonica* can feed on were explored. Furthermore, the growth of *K. japonica* and its ingestion rates of the dinoflagellate *Akashiwo sanguinea*—a suitable algal prey item—heterotrophic bacteria, and the cyanobacteria *Synechococcus* sp., as a function of prey concentration were determined. Among the prey tested, *K. japonica* ingested heterotrophic bacteria, *Synechococcus* sp., the prasinophyte *Pyramimonas* sp., the cryptophytes *Rhodomonas salina* and *Teleaulax* sp., the raphidophytes *Heterosigma akashiwo* and *Chattonella ovata*, and the dinoflagellates *Heterocapsa rotundata, Amphidinium carterae, Prorocentrum donghaiense*, *Alexandrium minutum*, *Cochlodinium polykrikoides*, *Gymnodinium catenatum*, *A. sanguinea*, *Coolia malayensis*, and the ciliate *Mesodinium rubrum*, however, it did not feed on the dinoflagellates *Alexandrium catenella*, *Gambierdiscus caribaeus*, *Heterocapsa triquetra, Lingulodinium polyedrum*, *Prorocentrum cordatum*, *P. micans,* and *Scrippsiella acuminata* and the diatom *Skeletonema costatum*. Many *K. japonica* cells attacked and ingested a prey cell together after pecking and rupturing the surface of the prey cell and then uptaking the materials that emerged from the ruptured cell surface. Cell of *A. sanguinea* supported positive growth of *K. japonica*, but neither heterotrophic bacteria nor *Synechococcus* sp. supported growth. The maximum specific growth rate of *K. japonica* on *A. sanguinea* was 1.01 d^{-1}. In addition, the maximum ingestion rate of *K. japonica* for *A. sanguinea* was 0.13 ng C $predator^{-1}d^{-1}$

(0.06 cells predator^{-1}d^{-1}). The maximum ingestion rate of *K. japonica* for heterotrophic bacteria was 0.019 ng C predator^{-1}d^{-1} (266 bacteria predator^{-1}d^{-1}), and the highest ingestion rate of *K. japonica* for *Synechococcus* sp. at the given prey concentrations of up to ca. 10^7 cells ml^{-1} was 0.01 ng C predator^{-1}d^{-1} (48 *Synechococcus* predator^{-1}d^{-1}). The maximum daily carbon acquisition from *A. sanguinea*, heterotrophic bacteria, and *Synechococcus* sp. were 307, 43, and 22%, respectively, of the body carbon of the predator. Thus, low ingestion rates of *K. japonica* on heterotrophic bacteria and *Synechococcus* sp. may be responsible for the lack of growth. The results of the present study clearly show that *K. japonica* is a predator of diverse phytoplankton, including toxic or harmful algae, and may also affect the dynamics of red tides caused by these prey species.

Prior to the present study, the phototrophic dinoflagellate *Heterocapsa minima* was not reported from Korean waters. I isolated this species from waters of Mijo Port, southern Korea in 2016. The genus *Heterocapsa* has been well documented as one of the major red-tide or harmful dinoflagellates. To investigate effective protist predators on *H. minima*, feeding by the engulfment-feeding heterotrophic dinoflagellates (HTDs) *Oxyrrhis marina*, *Gyrodinium dominans*, and *Polykrikos kofoidii*, the peduncle-feeding HTD *Pfiesteria piscicida*, the pallium-feeding HTD *Oblea rotunda*, and the naked ciliates *Pelagostrobilidium* sp. on *H. minima* was explored. I found that *O. marina*, *G. dominans*, *P. piscicida*, and

Pelagostrobilidium sp. were able to feed on *H. minima*. However, *H. minima* may not affect growth of predators. These findings suggest that the effect of predation by heterotrophic protists on *H. minima* might be negligible.

***Keywords*: Dinoflagellate, Protist, Feeding, Growth, Ingestion, Harmful algal bloom, Red tide**

Student Number: 2016-20404

Table of Contents

List of Tables

List of Figures

Chapter 1. General introduction

Marine heterotrophic nanoflagellates (HNFs) and dinoflagellates are major components in marine ecosystems (Patterson and Larsen, 1991; Sanders et al., 1992; Hansen, 2011; Berge et al., 2012; Stoecker et al., 2017; Lim et al., 2018). HNFs are known to be major predators of marine bacteria and occasionally control their populations (Fenchel, 1982; Azam et al., 1983; Sieburth, 1984; Tanaka et al., 1997; Seong et al., 2006) and in turn, they are prey for heterotrophic dinoflagellates, ciliates, and copepods (Verity, 1991; Nakamura and Turner, 1997; Jeong et al., 2007). Therefore, they play an important role in the transfer of bacterial materials to heterotrophic protists and metazoans in marine planktonic food webs, and thus are a key component in marine microbial loops (Azam et al., 1983).

The phototrophic dinoflagellates are important prey items for other mixotrophic dinoflagellates, heterotrophic dinoflagellates (Hansen, 1992), and several varieties of metazooplankton. Owing to their diverse and important roles in marine ecosystems, studies have suggested that they form one of the major functional groups (e.g., Mitra et al., 2016). Therefore, to understand the roles of phototrophic dinoflagellates in marine ecosystems, it is important to understand their predators among co-occurring plankton, and their growth rates caused by predation of the species implied in the predator-prey relationships of the targeted dinoflagellates (e.g., Jeong et al., 2015).

This thesis consists of 5 chapters including this introduction (Fig. 1). Overall, newly discovered role of the heterotrophic nanoflagellate *Katablepharis japonica* as an effective predator on red-tide organisms and the first report of the phototrophic dinoflagellate *Heterocapsa minima* in Korean waters and its interactions with heterotrophic protists.

In chapter 2, the distributions of the heterotrophic nanoflagellate *Katablepharis japonica* in Korean waters were analyzed using quantitative real-time PCR. The specific primers and probe for *K. japonica* were developed. Also, 24 samples in Jinhae Bay in May 2014 to July 2017 were analyzed. The results of this chapter provides on understanding relationships between the distribution of *K. japonica* and environmental factors.

In chapter 3, to investigate the feeding and ecological roles of major heterotrophic nanoflagellates *Katablepharis* spp., the feeding ability of *Katablepharis japonica* on bacteria and diverse algal prey species including red-tide species were explored. Furthermore, the growth of *K. japonica* and its ingestion rates of the dinoflagellate *Akashiwo sanguinea*, heterotrophic bacteria, and the cyanobacteria *Synechococcus* sp., as a function of prey concentration were determined. This characteristic, studied in this chapter, provided a basis for understanding the interactions between *Katablepharis* spp. and bacteria and phytoplankton and their ecological roles in marine ecosystems, specifically, in red-tide dynamics.

In chapter 4, prior to the present study, the phototrophic dinoflagellate *Heterocapsa minima* was not found in the Korean waters. I successfully isolated *H. minima* cells from Mijo port, southern Korea in 2016 and established a clonal culture of this species. Using this culture, I determined the molecular sequences of the D1-D2 LSU rDNA, and the ITS region (ITS1, 5.8S, and ITS2) and performed phylogenetic analyses. Furthermore, to investigate its protistan predators, interactions between *H. minima* and common heterotrophic protists were explored. This chapter provides a basis for understanding the interactions between *H. minima* and common heterotrophic protist species, and their ecological roles in the marine planktonic community.

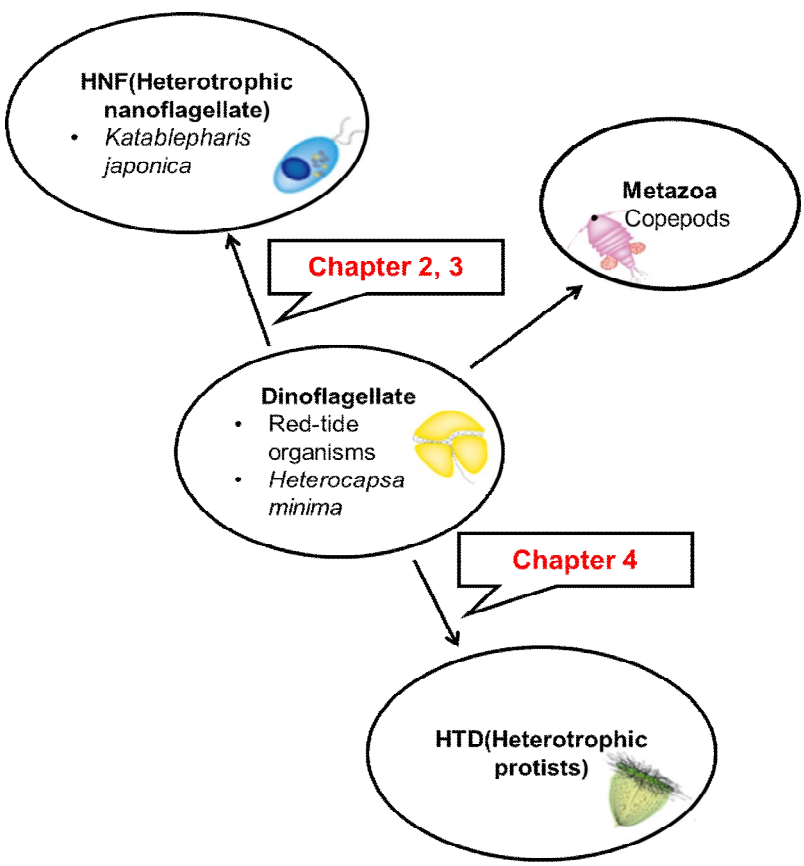

Fig. 1. Thesis Outline

Chapter 2. Distribution of the heterotrophic nanoflagellate *Katablepharis japonica* in Jinhae Bay, Korea in 2014-2017 using quantitative real-time PCR

2.1. Introduction

The genus *Katablepharis* is one of the major genera of HNFs and has a worldwide distribution (Kahn et al., 2014; Péquin et al., 2017). This genus was first established by Skuja in 1939 and placed in the family Katablepharidaceae in the class Cryptophyceae (Lee and Kugrens, 1991), however, it was moved to Katablepharidea, an independent class (Vørs, 1992; Clay and Kugrens, 1999; Okamoto and Inouye, 2005).

Recently, a free-living HNF was isolated from Masan Bay, Korea and a clonal culture was established. Based on morphological and genetic analyses, it was revealed to be *Katablepharis japonica*. The small subunit ribosomal DNA of this Korean strain was identical to that of a Japanese strain (GenBank accession number AB231617). Data on the distribution and population dynamics of *K. japonica* are lacking.

In this study, the distribution of *K. japonica* in Korean waters was analyzed using qRT-PCR assay utilizing TaqMan probes. Twenty four samples were collected in Jinhae Bay, Korea in May 2014 to July 2017. To detect specifically species, primers and probes were originally developed to fit the target *Katablepharis japonica* using sequences of its small subunit

ribosomal DNA regions. All these primers and probes passed the species-specificity test.

This study provides the comprehensive data on distribution of *Katablepharis japonica* in Jinhae Bay, Korea. The results of this study provide a basis on better understanding the ecology of the *K. japonica*, and relationships between the abundances of *K. japonica* and environmental factors.

2.2. Materials and Methods

2.2.1. The quantitative real-time PCR assay

To develop a probe and primer set for the detection and quantification *of Katablepharis japonica*, DNA of cells from a dense culture of *K. japonica* KJMS1610 was extracted using the AccuPrep® Genomic DNA Extraction Kit (Bioneer Cooperation, Daejeon, Korea). Then, the small subunit ribosomal DNA (SSU rDNA) region was amplified using EukA (Medlin et al., 1988) as the forward primer and G23R (Litaker et al., 2003) as the reverse primer (Table 1). PCR amplification and sequencing were conducted as in Lee et al. (2017). In addition to the obtained sequences of my *K. japonica*, the sequences of the other strains of *K. japonica* and related dinoflagellate SSU rDNA region available from GenBank were aligned using MEGA v.4 (Tamura et al., 2007). Manual curation of the alignments was conducted to identify unique sequences and develop a *K.*

japonica specific qPCR assay. The sequences for the primer-probe set were selected from the region that were conserved *K. japonica* strains, but allowed for discrimination from other dinoflagellates. The primer and probe sequences of the target species were analyzed using a method of Lee et al. (2017). The probe was dual-labeled with the fluorescent dyes FAM and BHQplus (Biosearch Technologies Inc., Novato, CA) at the 5' and 3' ends, respectively.

Table 1

Information on the primers used in this study.

Type	Name	Sequence (5'-3')	References
Forward primer	EukA	AACCTGGTTGATCCTGCCAGT	Medlin et al. 1988
Reverse primer	G23R	TTCAGCCTTGCGACCATAC	Litaker et al. 2003

A dense culture of *K. japonica* KJMS1610 was also used to conduct standard curve. The DNA was extracted from the dense culture of *K. japonica* and then diluting the extracted DNA in serial. To conduct standard curve, 2-l PC bottles that contain the dense culture (containing approximately > 1000 cells ml^{-1}) were well mixed and 10-ml aliquots were taken and fixed with 5% Lugol's iodine solution from bottle to enumerate cell concentrations. The determination of cell concentrations was examined under a compound microscope and enumerated in 1-ml SRC chamber.

The standard curve was conducted by serially diluting extracted DNA originated from a dense culture of *K. japonica* (concentration = 6,930 cells ml^{-1}) by adding diverse aliquots of extracted DNA to elution buffer so that each sample may target approximately 50000, 25000, 10000, 1000, 100, 10, and 1 cells ml^{-1} of *K. japonica* (Table 2). The whole procedure including DNA extraction and DNA dilution was conducted in triplicate. Then samples were stored at -20 ºC in the freezer and qPCR amplification was conducted within a day. The qPCR assays for determination of the standard curve obtained by preparation were performed as in Lee et al. (2017). The DNA of each sample was amplified 7–12 times to ensure accuracy of results and natural seawater samples without *K. japonica* cells were used as the negative control. The fluorescence of each reaction tube was quantified per cycle and the threshold for a positive reaction was automatically selected by using the default settings on the accompanying qPCR instrument using Rotor-Gene Q Series Software (Qiagen, Hilden, Germany). Then, based on the result obtained, the threshold of standard curves was fixed at 0.0138, which was first automatically selected by the software, and showed most optimal florescence results. From the threshold, the threshold cycle (Ct) values, which were the intersection between the amplification curve and threshold line, were obtained.

Table 2

Preparation methods used to determine standard curves used in this study to determine the efficiency of real-time PCR in respect to the quantification of the heterotrophic nanoflagellate *Katablepharis japonica*

Species	Collection date	Collection area	Temp. (℃)	Salinity	Actual cell concentration approximate (cells ml^{-1})
Katablepharis japonica	2016 10	Masan, Korea	21.8	19.3	50000, 25000, 10000, 1000, 100, 10, and 1

*: Cell concentration of the culture (6930 cells ml^{-1}).

2.2.2. Relationships between the abundance of K. japonica and environmental factors

Data were analyzed statistically using the IBM SPSS, Statistics v25 program. Pearson's correlation analysis was conducted for the correlation between the abundances of *K. japonica* and environmental factors. (Garson, 2013; Heck et al., 2013; West, 2009; West et al., 2014).

2.3. Results

2.3.1. Assay development

Primers and probe for *Katablepharis japonica* were established (Table 3). Specific primers and probe passed specificity test. Only reagents

containing target species were detected. Also, standard curve of *K. japonica* was developed and r2 value of curve is higher than 0.98.

Table 3

Species-specific primers and probe using sequences of the SSU rDNA regions

Type	Name	Sequence (5'-3')
Forward primer	JAPOF	TGCTTGTCGGCTCTTCTTTT
Reverse primer	JAPOR	GGCCTGCTTTGAACACTCTAA
Probe	JAPOP	GGGGACCACATTGCTCTTTACTGAGGA

2.3.2. Distribution of K. japonica in Korean waters assessed using qPCR

Among the 24 samples investigated in the present study, the abundance of *K. japonica* was $\geq$0.2 cells ml^{-1} in 12 samples in Jinhae Bay from May 2014 to July 2017 (Table 4). Cells of *K. japonica* were not detected in samples off of May, July 2014, May, September 2015, January, March, July, September, and October 2016. The highest abundance of *K. japonica* in Jinhae Bay, 13.6 cells ml^{-1}, was obtained in September 2014, while the second-highest abundance, 4.9 cells ml^{-1}, was measured in May 2017 (Table 4).

Table 4

The abundance of *Katablepharis japonica* (Kj), temperature (T), salinity (S), and chlorophyll-a concentration in Jinhae Bay, Korea

***Katablepharis japonica* (Kj)**				
date	**T**	**S**	**Chl-a (mg/m^3)**	**Kj (cells/ml)**
2014 0509	16.7	33.8		
2014 0522	19.3	32.8		
2014 0711	25.3	32.7		-
2014 0904	26.2	26.5	25.2	13.6
2014 0919	22.5	31.2		
2014 1111	17.7	32.8		0.4
2015 0119	6.5	33.5	4.0	0.6
2015 0409	12.6	31.2	2.7	0.2
2015 0528	22.2	32.2	7.4	-
2015 0716	21.7	30.2		0.7
2015 09				-
2015 0904	25.8	31.6	4.4	-
2015 1014	21.1	32.2	8.7	0.5
2016 0115	8.3	32.1	3.7	-
2016 0330	13.2	32.4	2.5	-
2016 0511	17.7	30.8	3.0	0.3
2016 0706	22.6	30.7	2.5	1.4
2016 0710				-
2016 0907	25.6	26.9	9.4	-
2016 1008	22.4	24.6	8.1	-
2016 1216	10.5	32.2	30.6	1.9
2017 0326	9.7	32.3		2.0
2017 0518	20.1	33.3		4.9
2017 0708	23.8	28.3		2.2

2.3.3. Relationships between the abundance of K. japonica, temperature, salinity, and chlorophyll-a concentration in Jinhae Bay, Korea.

The abundance of the heterotrophic nanoflagellate *Katablepharis japonica* in Jinhae Bay, Korea, together with environmental factors, were studied. Through the IBM SPSS program, the correlation between the abundances of *K. japonica* and chlorophyll-a appears to be significant at a significance level of $P < 0.05$. Also, it has a slightly higher correlation of around 0.634 (Table 5). Temperature and salinity concentrations correlated poorly with the abundances of *K. japonica*.

Table 5

Correlation between the abundance of *K. japonica* (kj), temperature (T), salinity (S), and chlorophyll-a (Chl-a) concentration in Jinhae Bay, Korea

Correlations					
		T	**S**	**Chl-a**	**Abundance of Kj**
T	Pearson Correlation	1	-.507*	.097	.226
	Sig. (2-tailed)		.022	.753	.339
	Covariance	40.565	-7.865	6.090	4.455
	N	20	20	13	20
S	Pearson Correlation	-.507*	1	-.257	-.318
	Sig. (2-tailed)	.022		.396	.172
	Covariance	-7.865	5.925	-6.291	-2.401
	N	20	20	13	20
Chl-a	Pearson Correlation	.097	-.257	1	.634*
	Sig. (2-tailed)	.753	.396		.020
	Covariance	6.090	-6.291	80.711	21.077
	N	13	13	13	13
Abundance of Kj	Pearson Correlation	.226	-.318	.634*	1
	Sig. (2-tailed)	.339	.172	.020	
	Covariance	4.455	-2.401	21.077	8.872
	N	20	20	13	22

*. Correlation is significant at the 0.05 level (2-tailed)

2.4. Discussion

2.4.1. Detection of Katablepharis japonica using quantitative real-time PCR assay

In this study, species-specific primers and probe for the qRT-PCR assay on *K. japonica* were developed. Sequences of SSU rDNA regions were used in this study to easily find unique sequences which only one species have. Also, the TaqMan method was chosen in this study to minimize the chance to detect false-positive signals. TaqMan probe method is more stable than SyBR Green method, because additional specific probe is needed in TaqMan method (Antonella and Luca, 2013).

2.4.2. Relationships between the abundance of K. japonica, temperature, salinity, and chlorophyll-a concentration in Jinhae Bay, Korea.

The abundance of *K. japonica* in this study was significantly affected by chlorophyll-a concentration, but not water temperature or salinity. The phototrophic dinoflagellates generally have chloroplasts (Dodge, 1971; Dodge, 1975; Gibbs, 1981). So this study suggests a significant relationship between the abundances of *K. japonica* and other phytoplankton. *K. japonica* may feed on co-occurring phytoplankton. Thus, it is worthwhile to investigate feeding by *K. japonica* on diverse algal prey items.

Chapter 3. Feeding by the heterotrophic nanoflagellate *Katablepharis japonica* on red-tide organisms

3.1. Introduction

In Chapter 2, the distribution of the HNF *Katablepharis japonica* was significantly affected by chlorophyll-a, indicating feeding by this HNF on phytoplankton. Compared with numerous studies on predation by HNFs on bacteria, there have been considerably fewer studies that have investigated HNF feeding on algal prey (e.g., Suttle et al., 1986; Kühn et al., 1996; Schnepf and Schweikert, 1997; Clay and Kugrens, 1999).

Marine phytoplankton is a major component of marine ecosystems and major primary producers in the sea, and in turn, it is an important prey item for diverse mixotrophic and heterotrophic organisms (Sanders, 1991; Stoecker, 1998; Tillmann, 2004; Jeong et al., 2010b, 2015; Lim et al., 2017). Some phytoplankton species are toxic or harmful to other marine organisms and humans (Smayda, 1997; Basti et al., 2016; Jeong et al., 2017). Furthermore, some species are primarily responsible for harmful algal blooms (HAB) or red tides, which cause large-scale mortality of fish or human illnesses (Hallegraeff, 1993; Anderson, 1989; Park et al., 2013; Lim et al., 2015; Reich et al., 2015; Lee et al., 2016; Grattan et al., 2016). Therefore, understanding population dynamics of a red tide or HAB species, and predicting the outbreaks, persistence, and declines of the red tide or

HAB species are critical concerns in scientists, officials, and people in the aquaculture industry. In population dynamics of a red tide or HAB species, growth and mortality caused by predation are two critical parameters (e.g., Jeong et al., 2015). Compared to the number of studies exploring the growth of a red tide species, those on mortality caused by predation are relatively rare (e.g., Turner, 2006; Jeong et al., 2010b, 2015). Furthermore, most reported predators of red tide organisms are heterotrophic dinoflagellates, ciliates, and metazoans (Hansen, 1991; Jeong et al., 2003, 2015; Tillmann, 2004; Kamiyama et al., 2006; Turner, 2006, 2014; Harvey and Menden-Duer, 2011; Kim et al., 2013; Yoo et al., 2013a. 2013b). Predation by free-living HNFs on red tide species is still poorly understood, although free-living HNFs and red tide species usually co-occur in most marine environments and the abundance of free-living HNFs in often greater than that of heterotrophic dinoflagellates, ciliates, and metazoans (Jeong et al., 2013; Yoo et al., 2013a). Therefore, it is worthwhile to explore feeding by HNFs on red tide species.

In marine environments, *Katablepharis* spp. sometimes dominate the assemblages of free-living HNFs (e.g., Kahn et al., 2014), however, there have been only a few studies on feeding by marine *Katablepharis* species (e.g., Clay and Kugrens, 1999). These studies briefly reported that *Katablepharis* spp. fed on the haptophyte *Chrysochromulina parva* and the cryptophytes *Chroomonas* sp. and *Rhodomonas* sp., however, many

common phytoplankton species, including harmful dinoflagellates and raphidophytes, have not yet been tested as prey for *Katablepharis* spp. Thus, it is worthwhile to explore the interactions between *Katablepharis* spp. and co-occurring phytoplankton and their ecological roles in marine planktonic communities.

In the present study, using this culture, the type of the prey that *K. japonica* can feed upon was investigated by providing them with heterotrophic bacteria, cyanobacteria, and diverse phytoplankton. Additionally, the growth of *K. japonica* and the ingestion rates of *K. japonica* on the harmful dinoflagellate *Akashiwo sanguinea*, the suitable prey, heterotrophic bacteria, and the cyanobacteria *Synechococcus* sp., as a function of prey concentration were determined. The results of the present study provided a basis for understanding the interactions between *Katablepharis* spp. and bacteria and phytoplankton and their ecological roles in marine ecosystems, specifically, in red tide dynamics.

3.2. Materials and Methods

3.2.1. Preparation of experimental organisms

Many algal species belonging to diverse taxa and having diverse sizes and shapes were provided as potential prey items (Table 6). Some species were thecate and others were non-thecate and single cells to chain forms. A

culture of *Alexandrium catenella* CCMP 1493 (previously *A. tamarense* CCMP 1493) that is a toxic strain was obtained from National Center for Marine Algae and Microbiota, USA (Orr et al., 2013). All algal prey species, except *Cochlodinium polykrikoides* and *Lingulodinium polyedra*, were grown at 20°C in enriched f/2-Si seawater media (Guillard and Ryther, 1962) under 20 μE m^{-2} s^{-1} illumination on a 14:10 h light/dark cycle. Cells of *C. polykrikoides* and *L. polyedra* were grown under continuous illumination of 50 μE m^{-2} s^{-1}, provided by a cool white fluorescent light, because they do not grow well under lower illumination on a light/dark cycle (Lee et al., 2014). The mean equivalent spherical diameter (ESD) ± standard deviation was measured using an electronic particle counter (Coulter Multisizer II; Coulter Corporation, Miami, Florida, USA). The ESD of the phytoplankton species were obtained from previous studies (Jeong et al., 2010a, 2011, 2012b, 2016; Yoo et al., 2010; Kang et al., 2011).

Table 6

Taxa, size, and concentration of bacterial and algal prey species offered to *Katablepharis japonica.* Mean equivalent spherical diameter (ESD, μm) for algae. The initial concentrations of *K. japonica* were 500–2000 cells ml^{-1}. T: Thecate, NT: Non-thecate, Y: Attack or feeding by *K. japonica*, N: Not attacked or fed on by *K. japonica*

Species	ESD (± SD)	Initial prey concentration (cells/ml)	Attack	Feeding by *K. japonica*
Bacteria				
Heterotrophic bacteria	1.0 (0.04)	$1x10^7$		Y
Synechococcus sp.	1.0 (0.2)	$1x10^7$		Y
Bacillariophytes				
Skeletonema costatum	5.9 (1.1)	30,000	Y	**N**
Prymnesiophytes				
Isochrysis galbana	4.8 (0.2)	150,000	Y	?
Prasinophytes				
Pyramimonas sp.	5.6 (0.1)	100,000	Y	Y
Cryptophytes				
Teleaulax sp.	5.6 (1.5)	50,000	Y	Y
Rhodomonas salina	8.8 (1.5)	50,000	Y	Y
Rhaphidophytes				
Heterosigma akashiwo	11.5 (1.9)	30,000	Y	Y
Chattonella ovata	40.0 (1.6)	2000	Y	Y

Dinoflagellates				
Heterocapsa rotundata (T)	5.8 (0.4)	100,000	Y	Y
Amphidinium carterae (NT)	9.7 (1.6)	30,000	Y	Y
Prorocentrum minimum (T)	12.1 (2.5)	5000	Y	**N**
Prorocentrum donghaiense (T)	13.3 (2.0)	5000	Y	Y
Heterocapsa triquetra (T)	15.0 (4.3)	1000	Y	**N**
Alexandrium lusitanicum (T)	20.4	2000	Y	Y
Scrippsiella trochoidea (T)	22.8 (2.7)	5000	Y	**N**
Cochlodinium polykrikoides (NT)	25.9 (2.9)	2000	Y	Y
Prorocentrum micans (T)	26.6 (2.8)	2000	Y	**N**
Akashiwo sanguinea (NT)	30.8 (3.5)	2000	Y	Y
Alexandrium tamarense (T)	32.6 (2.7)	1500	Y	**N**
Coolia maleyensis (T)	32.8	2000	Y	Y
Gambierdiscus caribaeus (T)	67.4	100	Y	**N**
Gymnodinium catenatum (NT)	33.9 (1.6)	100	Y	Y
Lingulodinium polyedrum (T)	38.2 (3.6)	1000	Y	**N**
Naked ciliate				
Mesodinium rubrum	22 (0.04)	5500	Y	Y

The abundances of the predator for each target prey were 2000–5000 cells ml^{-1}

?, questionable; ESD, mean equivalent spherical diameter (μm) ± SD of the mean was measured by an electronic particle counter (Coulter Multisizer II, Coulter Corporation, Miami, FL).

The heterotrophic bacterial cells that originated from a clonal culture of *Katablepharis japonica* were used after being fluorescently labeled, following Sherr et al. (1987). In this study, the fluorescently labeled bacteria (FLB) were mostly seen as rods (a cylinder) and rarely spherical. The longest (length) and the shortest axes (width) of 30 FLB cells were measured under an epifluorescence microscope as in Lee and Fuhrman (1987) and then the volume was calculated according to the following equation: volume = $[\pi (3L - W)/3 \times (W/2)^2]$ for a rod (cylinder) and $4/3 \times [\pi R^3]$ for a sphere, where L = length, W = width, and R = radius as in Lee (1993). The mean ($\pm$ standard error, n) volumes of FLB were 0.45 μm^3 ($\pm$ 0.05, n=30).

The cyanobacterium *Synechococcus* sp. (SYN, GenBank accession number = DQ023295, ESD = ca. 1 μm) were grown at 20°C in enriched f/2 seawater media (Guillard and Ryther 1962) without silicate, under a 14:10 h light-dark cycle of 20 $\mu E\ m^{-2}\ s^{-1}$ provided by a cool white fluorescent light (Table 6).

Cells of *K. japonica* were isolated from plankton samples collected in Masan Bay, Korea in October 2016, when the water temperature and salinity were 21.8°C and 19.3, respectively. The samples were screened gently through a 154-μm Nitex mesh and placed in 6-well tissue culture plates. A clonal culture of *K. japonica* KJMS1610 was established using two serial single-cell isolations. The raphidophyte *Chattonella ovata* was

originally provided as prey. As the concentration of *K. japonica* increased, the culture was sequentially transferred to 50-, 250-, and 800-ml flasks containing fresh prey (ca. 10,000 cells ml^{-1}), however, *Pyramimonas* sp. cells were not completely eliminated by the predator. Thus, *Akashiwo sanguinea* was provided as an alternative prey item because this prey was completely eliminated. The flasks were filled to capacity with freshly filtered seawater, capped, and placed on a shelf at 20°C under illumination of 20 μE m^{-2} s^{-1} provided by cool white fluorescent lights, under a 14:10 h light/dark cycle. The mean ESD of *K. japonica* was 8.1 μm and its carbon content was estimated from cell volume (Menden-Deuer and Lessard 2000) as 0.043 ng C per cell.

3.2.2. Feeding occurrence

Experiment 1 was designed to investigate the ability of *K. japonica* to feed on individual target species when unialgal diets of diverse algal species, *Synechococcus* sp., and heterotrophic bacteria were provided (Table 6). The initial concentrations of each algal species had a similar carbon biomass.

Algal prey

A culture of approximately 8000 cells ml^{-1} of *K. japonica* growing on *A. sanguinea* was transferred to a single 250-ml culture flask containing freshly filtered seawater after *A. sanguinea* became undetectable. This culture was maintained for 1 day. Three 1-ml aliquots were then removed

from the flask and examined with a light microscope to determine the concentration of *K. japonica.*

The initial concentrations of *K. japonica* (ca. 2000–5000 cells ml^{-1}) and each of the target algal species were established using an autopipette to deliver a predetermined volume of culture with a known cell density into wells of 6-well plate chambers. For each algal species, triplicate wells containing mixtures of *K. japonica* and prey (total of 5 ml in each well), and triplicate predator control wells containing a culture of *K. japonica* only (total of 5 ml in each well) were established. The plate chambers were placed on a shelf and incubated under a 14:10 h light-dark cycle of 20 μE m^{-2} s^{-1} of cool white fluorescent light.

After 2, 24, and 48 h, >30 *K. japonica* cells in the well were monitored under a dissecting microscope with a magnification of ×40–63 to determine whether *K. japonica* is able to feed on the target prey species.

Heterotrophic bacteria

For the epifluorescence microscopy, the heterotrophic bacterial cells that originated from a clonal culture of *K. japonica* were used after being fluorescently labeled as described above. To remove any aggregated FLB, the FLB were dispersed throughout the medium using a sonicator (Bransonic cleaner 5510E-DTH, Danbury, CT, USA) for 10–30 s and then filtered through 3-μm pore sized filter (Whatman, Polycarbonate, Maidstone, UK).

In this experiment, the initial concentrations of *K. japonica* (1000 cells ml^{-1}) and FLBs (1×10^7 cells ml^{-1}) were established using an autopipette to deliver a predetermined volume of culture with a known cell density to the experimental bottles. Triplicate 42-ml polycarbonate (PC) bottles (mixtures of predators and FLBs) and triplicate predator control bottles (containing predator only) were established at a single prey concentration. The bottles were placed on a shelf and incubated at 20°C under a continuous illumination of 20 μE m^{-2} s^{-1} provided by cool white fluorescent light. At the beginning, and after 5- and 10-min incubation periods, 5-ml aliquots were removed from each bottle, transferred into 20-ml vials, and then fixed with borate-buffered formalin [final conc. = 4% (v/v)] for FLB observation. The fixed samples were stained using 4′6′-diamidino-2-phenylindole (DAPI; final conc. = 1 μM) and then filtered onto 3 μm-pore-sized PC white membrane filters. Cells of *K. japonica* on the membranes were observed under an epifluorescence microscope (Ziess-Axiovert 200M, Carl Zeiss Ltd., Göttingen, Germany) at a magnification of 1000× and pictures were taken.

Cyanobacterial prey

A dense culture of *K. japonica* was transferred to a 1-l PC bottle containing freshly filtered seawater. Three 1-ml aliquots were then removed from the bottle and examined using a compound microscope to determine the *K. japonica* concentration.

In this experiment, the initial concentrations of *K. japonica* (1000 cells ml^{-1}) and *Synechococcus* (1×10^7 cells ml^{-1}) were established using an autopipette to deliver a predetermined volume of culture with a known cell density to the experimental bottles. Triplicate 42-ml PC bottles (mixtures of predator and *Synechococcus*) and triplicate predator control bottles (containing predator only) were established at a single prey concentration. The bottles were filled to capacity with freshly filtered seawater, capped, and placed on a shelf at 20°C under continuous illumination of 20 μE m^{-2} s^{-1}. After 5- and 10-min incubation, a 5-ml aliquot was removed from each bottle, transferred into a 20-ml vial, and fixed with formalin (final conc. = 4%). The fixed aliquots were filtered onto 3 μm-pore sized, 25-mm PC black membrane filters and then the concentrated cells on the membranes were observed under an epifluorescence microscope (Ziess-Axiovert 200M, Carl Zeiss Ltd., Göttingen, Germany) with red light excitation at a magnification of 1000× to determine whether *K. japonica* predator could feed on *Synechococcus*. Pictures showing ingested *Synechococcus* cells inside the protoplasm of each *K. japonica* cell were taken using a digital camera at a magnification of 1000×.

3.2.3. Feeding behaviors

Experiment 2 was designed to investigate the feeding behavior of *K. japonica* when provided with unialgal diet of the algal prey. The initial

concentrations of predator and prey used in Experiment 2 were the same as those described above for Experiment 1 (Table 6, 7).

Table 7

Design of experiments. The numbers in prey and predator columns are the actual initial densities (cells ml^{-1}) of prey and predators in Experiments 1–7 (see text). Values in parentheses in the predator column are the predator densities in the predator control bottles (prey density = 0 cells ml^{-1}). BI: Bottle incubation method. IC: Inclusion method

Expt	Prey		Predator		Method
No.	Species	Density	Species	Density	
1	Diverse prey	See Table 1	*Katablepharis japonica*	See Table 1	BI
2	Diverse prey	See Table 1	*K. japonica*	See Table 1	BI
3	*Akashiwo snaguinea*	16, 55, 79, 112, 664, 1089, 1928, 3305, 0	*K. japonica*	20, 35, 79, 74, 354, 836, 2356, 3253, (87)	BI
4	Heterotrophic bacteria	$1.1x10^5$, $1.3 x10^5$, $5.0 x10^5$, $1.0 x10^6$, $5.0 x10^6$, $7.1 x10^6$, $1.0 x10^7$	*K. japonica*	1000	IC
5	*Synechococcus* sp.	$4.1x10^5$, $9.5 x10^5$, $1.4 x10^6$, $1.9 x10^6$, $5.5 x10^6$, $6.7 x10^6$, $9.8 x10^6$	*K. japonica*	1000	IC
6	Heterotrophic bacteria	$6.9 x10^6$, $1.1 x10^7$	*K. japonica*	2950, 3700	BI
7	*Synechococcus* sp.	$7.3 x10^6$, $9.7 x10^6$	*K. japonica*	2290, 2340	BI

For each target species, a well containing a mixture of *K. japonica* and the prey (total of 5-ml) was established. As soon as the mixture was added to the well, many *K. japonica* cells attacked a prey cell together. Thus, the feeding processes, from the time a prey cell was attacked to the time the prey was completely ingested by the predators, were observed by monitoring the behavior of many unfed *K. japonica* cells for each prey species under a light microscope at a magnification of ×100–630. The feeding process for a *K. japonica* cell was documented using a video analyzing system (Sony DXC-C33; Sony Co., Tokyo, Japan) mounted on a compound microscope at a magnification of ×100–630.

To determine whether *K. japonica* can feed on actively swimming *Akashiwo sanguinea* cells, *K. japonica* cells were monitored after ca. 200 *K. japonica* cells and ca. 3000 *A. sanguinea* cells were mixed in two wells of a 12-well plate chamber. The feeding process of *K. japonica* cells feeding on 3 actively swimming *A. sanguinea* cells was documented using a video analyzing system. Furthermore, to determine whether *K. japonica* can feed on *A. sanguinea* cells when the concentration of the predator is low, *K. japonica* cells were monitored after establishing mixtures of *K. japonica* and *A. sanguinea* cells with predator:prey ratios of 10:100 (cells ml^{-1}:cells ml^{-1}), 20:500, 50:800, 100:1000, 200:2000, 500:3000, and 1000:4000 in wells of 12-well plate chambers. Duplicate wells for each ratio were established. The

feeding process for *K. japonica* cells feeding on actively swimming *A. sanguinea* cells was documented. Moreover, to examine whether *K. japonica* can feed on *A. sanguinea* cells under turbulent conditions, feeding by *K. japonica* cells on *A. sanguinea* was examined under a dissecting microscope after mixtures of *K. japonica* and *A. sanguinea* cells at predator:prey ratios of 100:1000 (cells ml^{-1}:cells ml^{-1}) and 1000:4000 had been established in one 42-ml flask for each ratio and subsequently placed on a rotating wheel for 3 h at 0.9 rpm.

3.2.4. Growth and ingestion rates as a function of prey concentration

Experiments 3, 4, and 5 were designed to measure the growth and ingestion rates of *K. japonica* on *A. sanguinea*, heterotrophic bacteria, and *Synechococcus* sp., as a function of prey concentration (Table 7). In the preliminary test, *K. japonica* grew well on *A. sanguinea*, but did not grow on the other algal prey species.

For the experiment on *A. sanguinea* prey (i.e., experiment 3), cultures of ca. 11,000 cells ml^{-1} of *K. japonica* growing on *A. sanguinea* were transferred to a single 250-ml culture flask containing freshly filtered seawater after *A. sanguinea* became undetectable. This culture was maintained for 1 day. Three 1-ml aliquots were then collected from the flask

and examined using a light microscope to determine the concentration of *K. japonica.*

The initial concentrations of *K. japonica* and *A. sanguinea* were established using an autopipette to deliver predetermined volumes of known cell concentrations to the flasks. For each predator-prey combination, triplicate experimental 50-ml culture flasks (containing a mixture of predator and prey) and triplicate control flasks (containing a culture of prey only) were established. Triplicate control flasks containing only *K. japonica* were also established at a single predator concentration. To ensure similar water conditions, the water of the predator culture was filtered through a 0.7-μm GF/F filter, and this was added to the prey control flasks at the same volume that the predator culture was added into the experimental flasks for each predator-prey combination. The flasks were filled to 10 ml with freshly filtered seawater, capped, and then placed on a shelf at 20 ^{o}C under a 14:10 h light-dark cycle of 20 μE m^{-2} s^{-1} of cool white fluorescent light. To determine the actual initial predator and prey densities (cells ml^{-1}) at the beginning of the experiment (Table 7) and after a 2-day incubation period, 5-ml aliquots were removed from each flask and fixed with 5% Lugol's solution. Then, all *K. japonica* cells and all or >300 prey cells in three 1-ml Sedgwick-Rafter chambers (SRC) were enumerated. Only 5 ml water in each 50-ml flask after subsampling at the beginning of the experiment was

incubated to increase encounter rates between predators and prey because *K. japonica* swam near the bottom of the flask (i.e., to create a shallow depth in the flasks).

The specific growth rate of *K. japonica* was calculated as follows:

$$\mu = \frac{\text{Ln}\,(C_t / C_0)}{t} \qquad (1)$$

where C_0 is the initial concentration of *K. japonica* and C_t is the final concentration after time t. The period was 2 days. The mean prey concentration was calculated using the equation of Frost (1972). The ingestion and clearance rates were calculated using the equations of Frost (1972) and Heinbokel (1978).

Data for *K. japonica* growth rate were fitted to the following equation:

$$\mu = \frac{\mu_{max}\ (x - x')}{K_{GR} + (x - x')} \qquad (2)$$

where μ_{max} is the maximum growth rate (day^{-1}), x is the prey concentration (cells ml^{-1} or ng C ml^{-1}), x' is the threshold prey concentration (i.e., the prey concentration where $\mu = 0$), and K_{GR} is the prey concentration sustaining 1/2 μ_{max}. Data were iteratively fitted to the model using DeltaGraph (SPSS Inc., Chicago, IL, USA).

Ingestion rate data were fitted to a Michaelis-Menten equation:

$$IR = \frac{I_{max}(x)}{K_{IR} + (x)} \quad (3)$$

where I_{max} is the maximum ingestion rate (cells predator^{-1} d^{-1} or ng C predator^{-1} d^{-1}), x is the prey concentration (cells ml^{-1} or ng C ml^{-1}), and K_{IR} is the prey concentration sustaining 1/2 I_{max}.

For the experiment on heterotrophic bacteria prey (i.e., experiment 4), one or two days prior to this experiment, the bacterial cells, which originated from a clonal culture of *K. japonica*, had been fluorescently labeled, as described above. To remove any aggregated FLB, the FLB were sonicated and then filtered through a 3-μm pore sized filter, as described above. The volumes of FLBs were measured as described above and the ratio of the actual initial abundances of FLBs to the abundances of non-FLB bacteria was also measured.

A dense culture of *K. japonica* growing on algal prey and then starved for 1 day (until ingested prey cells were undetected inside the protoplasm of the predator cells) was transferred into a 1-l PC bottle. Three 1-ml aliquots from the bottle were counted using a compound microscope to determine the cell concentrations of *K. japonica*, as described above. The mean actual initial predator and prey concentrations are shown in Table 6. Triplicate 42-ml PC experimental bottles (containing mixtures of predator and prey) and triplicate predator control bottles (containing predator only) were also

established. All the bottles were filled to capacity with freshly filtered seawater, capped, placed on a shelf, and incubated at 20°C under continuous illumination of 20 μE m^{-2} s^{-1} provided by cool white fluorescent lights. After 1-, 5-, 10-, and 20-min incubation periods, 5-ml aliquots were removed from each bottle, transferred into 20-ml vials, and fixed with borate buffered formalin [final conc. = 4% (v/v)]. The fixed samples were stained using DAPI (final conc. = 1 μM) and then filtered onto 3 μm-pore-sized PC white membrane filters. The FLB inside a *K. japonica* cell were enumerated under an epifluorescence microscope with blue light excitation. Additionally, at the beginning of the experiment, a 1-ml fixed aliquot was stained with DAPI and then filtered onto 0.2 μm-pore-sized PC black membrane filters. Bacteria (both FLB and non-FLB) outside *K. japonica* cells were also enumerated under an epifluorescence microscope with UV light excitation for non-FLB, and blue light excitation for FLB. After subsampling, the bottles were capped, placed on a shelf, and incubated again, as described above.

The ingestion rate of *K. japonica* on FLBs (FLBs $predator^{-1}$ h^{-1}) was calculated by linear regression of the number of FLBs per *K. japonica* cell as a function of incubation time as described by Sherr et al. (1987). Furthermore, the ingestion rate of *K. japonica* on heterotrophic bacteria (bacterial cells $predator^{-1}$ h^{-1}) was calculated by multiplying the ingestion

rate of *K. japonica* on FLBs by the ratio of the abundance of total heterotrophic bacteria (i.e., FLB plus non-FLB) relative to that of FLBs. All ingestion rate data were fitted to a Michaelis-Menten equation. In this plotting, the prey concentration is the sum of living heterotrophic bacteria (i.e., non-FLB) and FLBs.

For the experiment on *Synechococcus* prey (i.e., experiment 5), the initial concentrations of the *K. japonica* predator and live *Synechococcus* were established using an autopipette to deliver predetermined volumes of known cell concentrations to the bottles (Table 7). Triplicate 42-ml PC experimental bottles (containing mixtures of predator and prey) and triplicate predator control bottles (containing predator only) were also established. All the bottles were then filled to capacity with freshly filtered seawater, capped, and placed on the shelf. After 1-, 10-, and 20-min incubation, 5-ml aliquots were removed from each bottle, transferred into 20-ml vials, and then fixed with formalin (final conc. = 4%). One 2-ml fixed aliquot was filtered onto 3 μm-pore sized, 25 mm PC black membrane filters. Red-colored inclusions (*Synechococcus* cells) inside the protoplasm of >40 *K. japonica* predator cells on the PC black membrane filters were enumerated under an epifluorescence microscope with blue light excitation. No red-colored inclusions were observed inside the protoplasm of the *K. japonica* predators in the control bottles. The bottles were capped, placed on

a shelf, and incubated as described above. A linear regression curve for the number of prey cells inside a *K. japonica* predator cell against incubation time was obtained and then an ingestion rate (prey cells predator^{-1} h^{-1}) was calculated by extrapolation, as in Sherr et al. (1987).

Experiment 6 was designed to investigate whether heterotrophic bacteria alone support positive growth of *K. japonica*. The growth rates of *K. japonica* on living heterotrophic bacteria at two high bacterial concentrations were measured (Table 7).

One day before this experiment was conducted, a dense culture of *K. japonica* growing on algal prey, was transferred into a 1-l PC bottle containing filtered autoclaved seawater. Three 1-ml aliquots were then collected from the bottle and cells were enumerated to determine the concentration of *K. japonica*.

Initial concentrations of *K. japonica* and bacteria were established using an autopipette to deliver predetermined volumes of known cell concentrations to the flasks. Triplicate 50-ml experimental flasks (mixtures of predator and prey) and triplicate control flasks (prey only) were established for each predator-prey combination. All the flasks were then filled to capacity with autoclaved seawater, filtered by a 0.2-µm PC membrane filter (Chisso filter Co. LTD., Tokyo, Japan), and capped. To determine the actual initial predator and prey densities at the beginning of

the experiment and after 48-h incubation, a 5-ml aliquot was removed from each flask and fixed with 5% Lugol's solution. All or >300 *K. japonica* cells, fixed in Lugol's solution, in three 1-ml Sedgwick-Rafter counting chambers were enumerated. Another 5-ml aliquot was removed from each flask, fixed with formalin (final conc. = 4%), and filtered onto 0.2 μm-pore sized PC black membrane filters. The bacteria were enumerated, as described above. The specific growth rate μ (d^{-1}) of *K. japonica* was calculated as described above.

Experiment 7 was designed to investigate whether *Synechococcus* sp. supported positive growth of *K. japonica*. The growth rates of *K. japonica* on living *Synechococcus* sp. at two high bacterial concentrations were measured (Table 7).

The initial concentrations of the *K. japonica* predator and live *Synechococcus* sp. were established using an autopipette to deliver predetermined volumes of known cell concentrations to the flasks. Triplicate 50-ml PC experimental flasks (containing mixtures of predator and prey), triplicate prey control flasks (containing prey only), and triplicate predator control flasks (containing predator only) were also established. All the flasks were then filled to capacity with freshly filtered seawater, capped, placed on the shelf, and incubated at 20°C under an illumination of 20 μE m^{-2} s^{-1}. To determine the actual initial predator and prey densities at the

beginning of the experiment and after 48-h incubation, a 5-ml aliquot was removed from each bottle and fixed with 5% Lugol's solution. All or >300 *K. japonica* cells, fixed in Lugol's solution, in three 1-ml Sedgwick-Rafter counting chambers were enumerated. Another 5-ml aliquot was removed from each bottle, fixed with formalin (final conc. = 4%), and filtered onto 0.2 μm-pore sized PC black membrane filters. Red-colored prey cells on the PC filter were enumerated under an epifluorescence microscope. Growth rates were calculated as described above.

3.3. Results

3.3.1. Feeding occurrences

Among the bacterial and algal prey tested, *Katablepharis japonica* ingested heterotrophic bacteria, *Synechococcus* sp., the prasinophyte *Pyramimonas* sp., the cryptophytes *Rhodomonas salina* and *Teleaulax* sp., the raphidophytes *Heterosigma akashiwo* and *Chattonella ovata*, and the phototrophic dinoflagellates *Heterocapsa rotundata, Amphidinium carterae, Prorocentrum donghaiense*, *Alexandrium minutum* (previously *A. lusitanicum*), *Cochlodinium polykrikoides*, *Gymnodinium catenatum*, *Coolia malayensis*, and *A. sanguinea*, and the mixotrophic ciliate *Mesodinium rubrum* (Table 6; Figs. 2–4).

Under epifluorescence microscopy, an unfed *K. japonica* cell appeared to have a bright blue color in the center of the cell, but a thin blue color in the remaining parts (Fig. 2A). Furthermore, un-ingested FLBs appeared as bright blue colored rods (Fig. 2B). Many FLBs (seen as bright blue colored rods) were observed inside the protoplasm of a *K. japonica* cell (Fig. 2C).

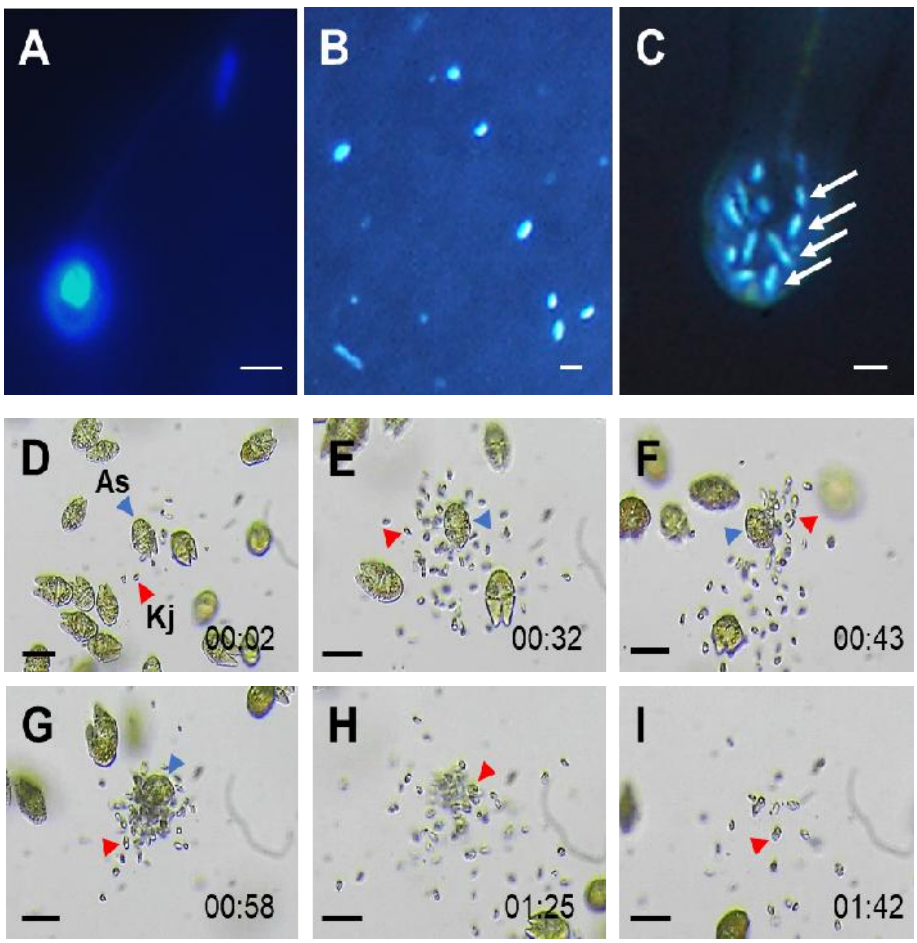

Fig. 2. Images of *Katablepharis japonica* cells feeding on bacteria and the dinoflagellate *Akashiwo sanguinea*. (A-C) Fluorescent labeled bacteria (FLB) prey. *K. japonica* cell without added prey observed under a light microscope (A), unfed FLBs (B), and many FLBs (arrows) inside the protoplasm of a *K. japonica* cell observed under an epifluorescence microscope (C). (D-I) Feeding process of *Katablepharis japonica* on *Akashiwo sanguinea* recorded by video-microscopy. (D-E) Several *K. japonica* (Kj) cells attacking an *A. sanguinea* cell (As). (F-H) Size of *A. sanguinea* cell reduced because of predation by Kj cells. (I) The *A. sanguinea* cell was undetectable. The numbers are min:s. Scale bar = 5 μm for (A, D-I), 1 μm for (B, C).

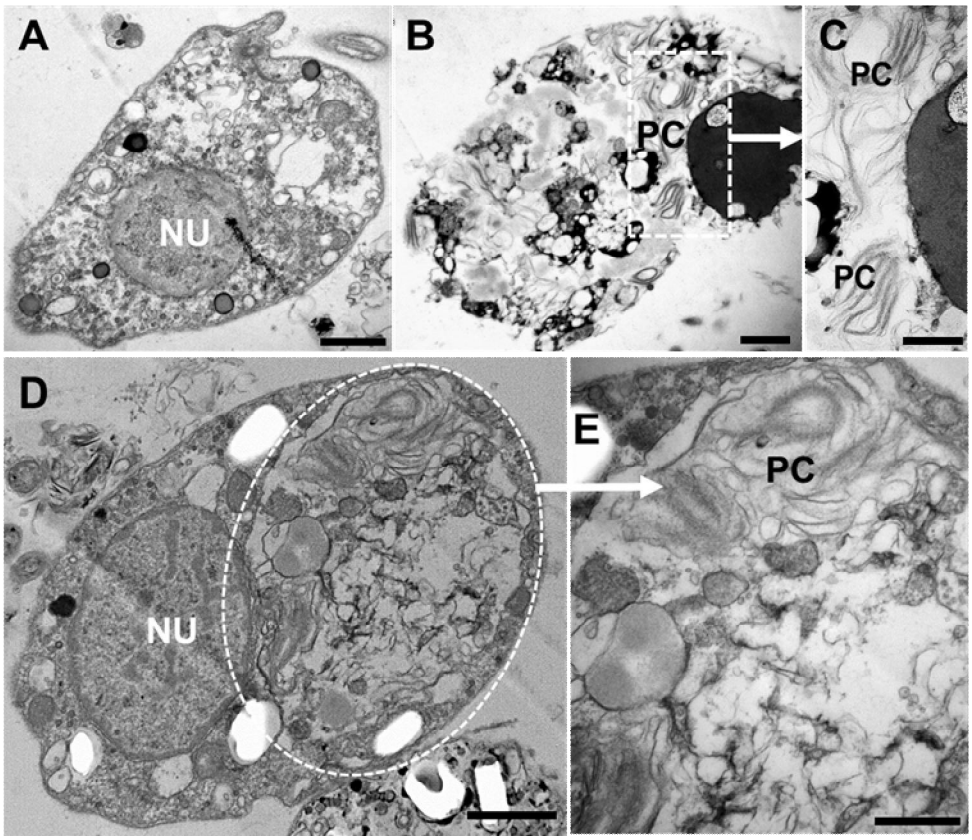

Fig. 3. Images of *Katablepharis japonica* cells feeding on the dinoflagellate *Akashiwo sanguinea* taken using a transmission electron microscope (A–E). (A) Unfed Kj cell containing the nucleus (Nu) in the center of the cell. (B) Intact As cell having chloroplast (PC). (C) Enlarged from (B). (D) A Kj cell contained ingested parts of As cells. The Nu descended to the posterior of the cell. (E) Enlarged from (D). Chloroplasts of As cells were observed. Scale bar = 0.5 μm for (C, E) and 1 μm for (A, B, D).

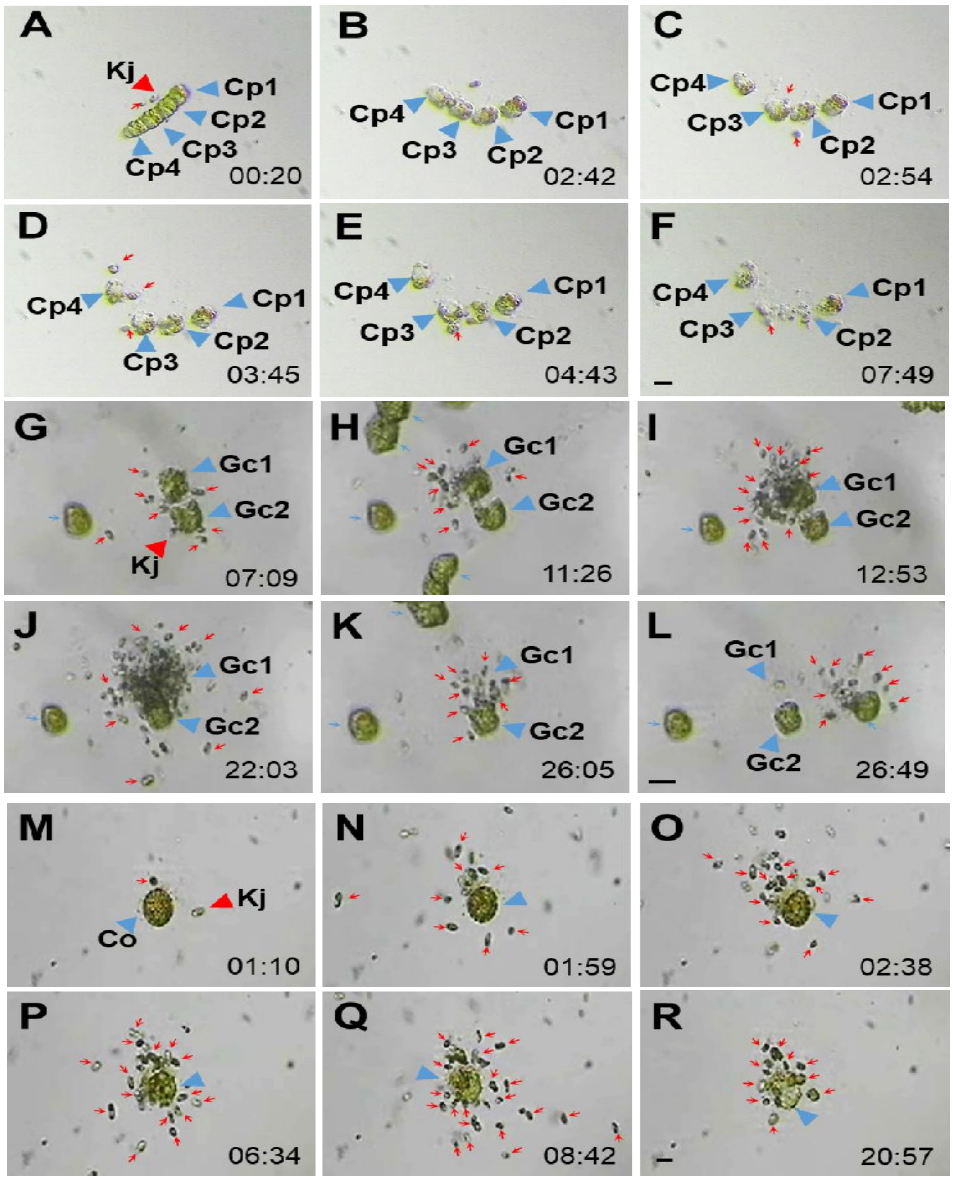

Fig. 4. Feeding process of *Katablepharis japonica* on the dinoflagellates *Cochlodinium polykrikoides* cells in a chain (A-F) and *Gymnodinium catenatum* cells in a chain (G-L) and the raphidophyte a *Chattonella ovata* cell (M-R) recorded by video-microscopy. (A) Several *K. japonica* (Kj) cells attacked a *C. polykrikoides* chain (Cp). (B-F) The chain of *C. polykrikoides* cells was broken and the cells decomposed because of predation by Kj cells. (G-J) Many Kj cells attacked *G. catenatum* (Gc) cells in a chain. (K, L) A Gc cell disappeared. (M-R) Many Kj cells attacking a *C. ovata* (Co) cell. The numbers are min:s. Scale bar = 5 μm.

Using transmission electron microscopy (TEM), unfed *K. japonica* cells were observed to have the nucleus in the center of their cells, and did not have chloroplasts (Fig. 3A). Intact *A. sanguinea* cells were observed to possess chloroplasts (Fig. 3B, C). *K. japonica* cells were observed to have a food vacuole containing parts of an *A. sanguinea* cell, such as chloroplasts (Fig. 3D, E). Inside the food vacuole, thylakoids, which are major components of a chloroplast, were clearly observed.

A few *K. japonica* cells attacked an algal prey cell or a ciliate cell, although many *K. japonica* cells approached and attacked together (Figs. 2, 4). After a few *K. japonica* cells attacked an algal prey cell, the attacked algal prey cells almost disappeared within ca. 40-70 s for *Akashiwo sanguinea*, *Mesodinium rubrum*, and *Rhodomonas salina* (Fig. 2D-I). Furthermore, *Gymnodinium catenatum* and *Chattonella ovata* cells disappeared within 1200-1600 s after a few *K. japonica* cells attacked the algal prey cell (Fig. 4G-R). Moreover, the time from which an algal prey cell was attacked by several *K. japonica* cells to that which the algal prey cell disappeared were 120-470 s for *C. polykrikoides*, *H. rotundata*, *P. donghaiense, A. carterae,* and *H. akashiwo,* (Fig. 4A-F).

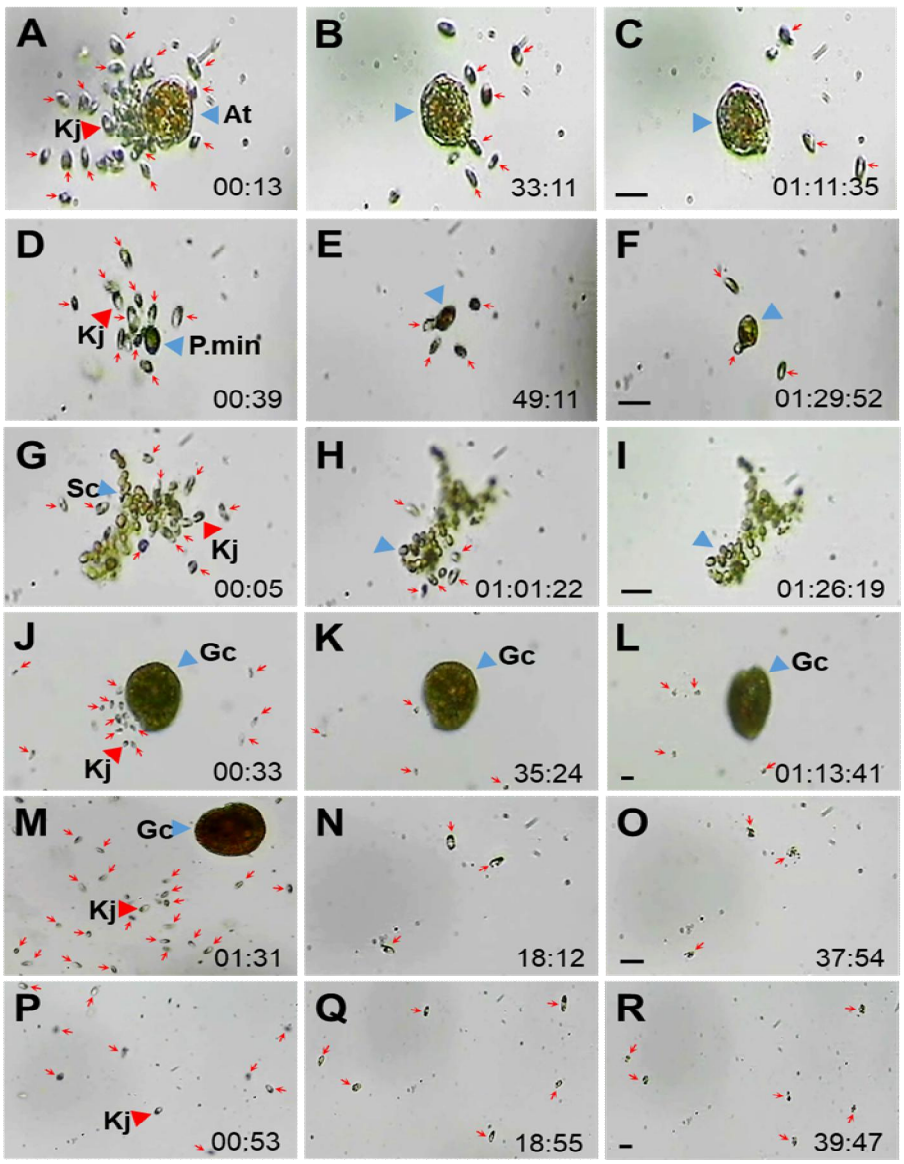

Fig. 5. The dinoflagellate and diatom species that *Katablepharis japonica* did not feed on, and lysis of Kj cells with addition of cells and culture filtrate of *Gambierdiscus caribaeus* (Gc). (A-C) *K. japonica* (Kj) cells attaching an *Alexandrium tamarense* (At) cell for ca. 70 min, but the At cell was not fed. (D–F) Kj cells attaching a *Prorocentrum minimum* (P.min) cell for ca. 90 min, but the P.min cell was not fed. (G–I) *K. japonica* (Kj) cells attaching a *Skeletonema costatum* (Sc) cell for ca. 85 min, but the Sc cell remained unchanged. (J-L) Kj cells attaching a Gc cell for ca. 80 min, but the Gc cell survived. (M–O) Lysis of Kj cells after addition of Gc cells. Almost all Kj cells were lysed at ca. 37 min. (P-R) Lysis of Kj cells after addition of Gc culture filtrate. Almost all Kj cells were lysed at ca. 40 min. The numbers are min:s. Scale bar = 5 µm.

Cells of *K. japonica* did not feed on the dinoflagellates *Gambierdiscus caribaeus*, *Heterocapsa triquetra, Lingulodinium polyedra, Prorocentrum cordatum* (previlusly *P. minimum*), *P. micans, Alexandrium catenella* CCMP 1493, and *Scrippsiella acuminate* (*S. trochoidea*), and the diatom *Skeletonema costatum* (Table 6; Fig. 5A-R). *K. japonica* cells were observed to attack (i.e., peck) these prey cells for >1 h, but the surface of these prey cells did not rupture. *K. japonica* cells were immobilized within 1 h after *G. caribaeus* cells or culture filtrates were added (Fig. 5M-R).

Cells of *K. japonica* were observed to feed on actively swimming *Akashiwo sanguinea* cells (Fig. 2G-L). Furthermore, *K. japonica* cells fed on actively swimming *A. sanguinea* cells at predator concentrations $\geq$100 cells ml^{-1}, but it did not feed on actively swimming *A. sanguinea* cells at predator concentrations of 10–50 cells ml^{-1}. Moreover, *K. japonica* fed on *A. sanguinea* cells under turbulent conditions.

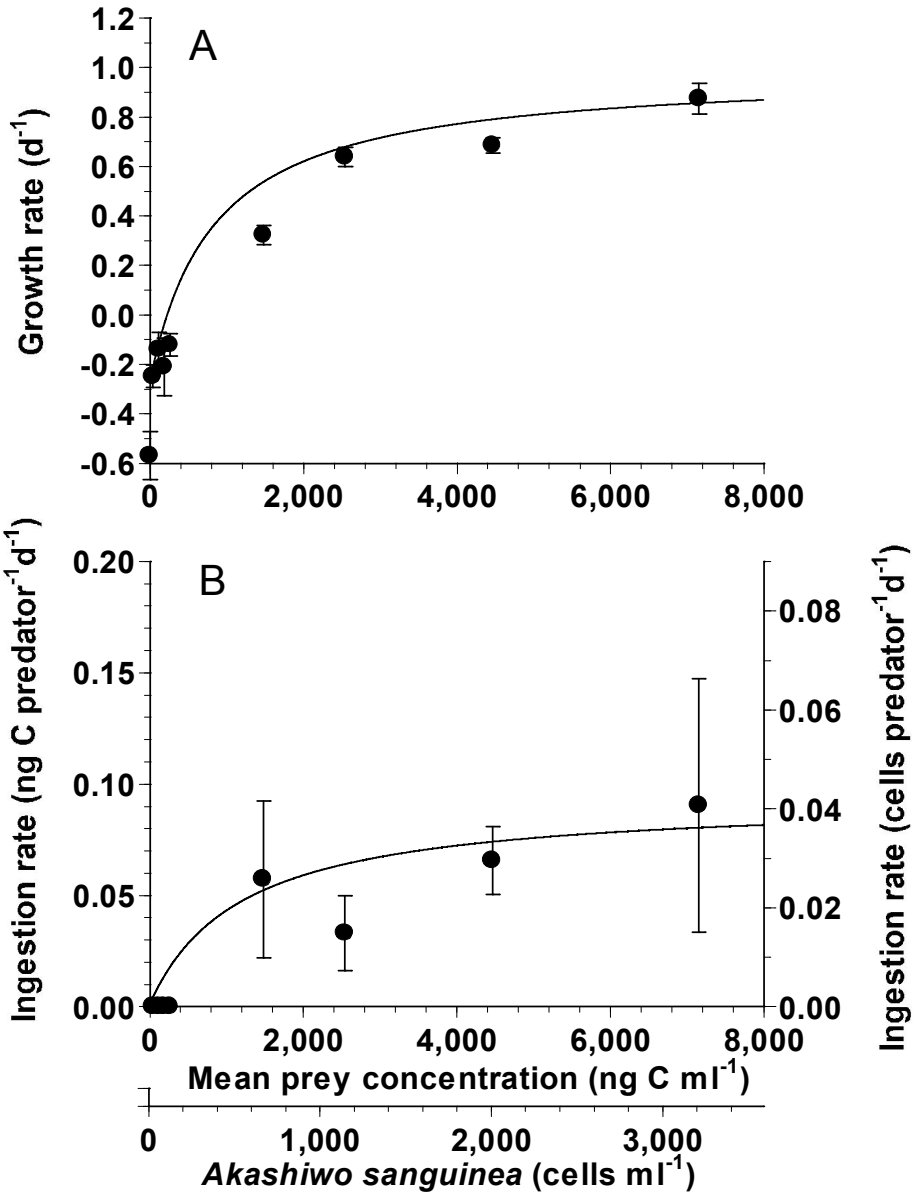

Fig. 6. Specific growth (A) and ingestion (B) rates of *Katablepharis japonica* on *Akashiwo sanguinea* as a function of mean prey concentration (x, ng C ml^{-1}). Symbols represent treatment means ± standard error. The curve in (A) is fitted by a Michaelis-Menten equation [Eq. (2)] using all treatments in the experiment. Growth rate (GR, d^{-1}) = 1.01 [(x - 425) / (1510 + (x - 425))], r^2 = 0.924. The curve in (B) is fitted by a Michaelis-Menten equation [Eq. (3)] using all treatments in the experiment. Ingestion rate (IR, ng C predator^{-1} d^{-1}) = 0.132 [x / (4090 + x)], r^2 = 0.417.

3.3.2. Growth and ingestion of K. japonica on algal prey

With increasing mean prey concentration, the specific growth rate of *K. japonica* on *Akashiwo sanguinea* increased rapidly at the prey concentrations <2540 ng C ml^{-1} (ca. 1140 cells ml^{-1}), but became saturated at higher prey concentrations (Fig. 6A). When the data were fitted to Eq. (2), the maximum specific growth rate of *K. japonica* feeding on *A. sanguinea* was 1.01 d^{-1}, whereas the growth rate without added prey was -0.57 d^{-1}. The threshold prey concentration (i.e., the prey concentration where $\mu = 0$) and K_{GR} (i.e., the prey concentration sustaining 1/2 μ_{max}) was 425 ng C ml^{-1} and 1510 ng C ml^{-1}, respectively.

With increasing mean prey concentration, the ingestion rate of *K. japonica* on *A. sanguinea* increased rapidly at prey concentrations <1480 ng C ml^{-1} (663 cells ml^{-1}), but increased slowly at higher prey concentrations (Fig. 6B). When the data were fitted to Eq. (3), the maximum ingestion rate of *K. japonica* on *A. sanguinea* was 0.13 ng C $predator^{-1}$ d^{-1} (0.06 cells $predator^{-1}$ d^{-1}), whereas the maximum clearance rate of *K. japonica* on *A. sanguinea* was 0.002 µl $predator^{-1}$ h^{-1}.

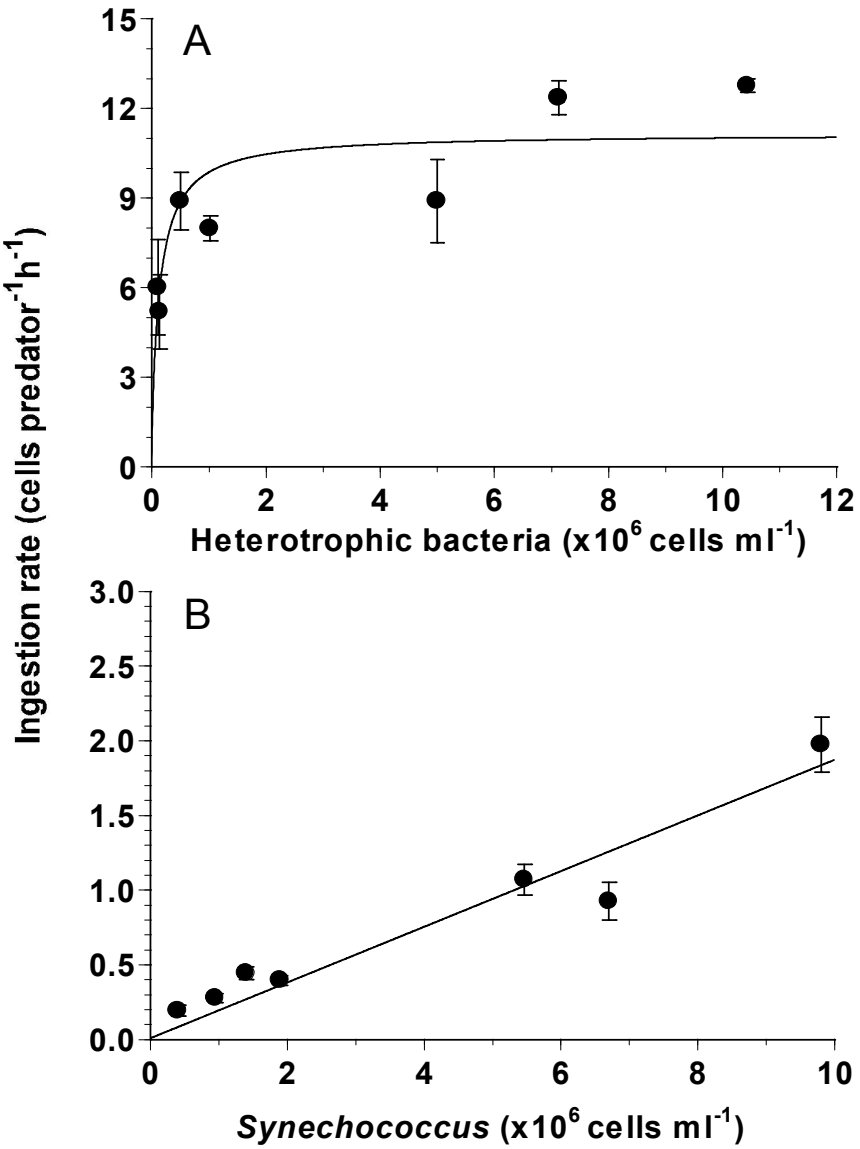

Fig. 7. Ingestion rates by *Katablepharis japonica* on heterotrophic bacteria (A) and the cyanobacterium *Synechococcus* sp. (B) as a function of mean prey concentration (pc, cells ml^{-1}). Symbols represent treatment means ± standard error. The curve in (A) is fitted by a Michaelis–Menten equation [Eq. (3)] using all treatments in the experiment. Ingestion rate (IR, cells $predator^{-1}$ h^{-1}) = 11.1 [pc / (0.13×10^6 + pc)], $r^2 = 0.558$. The curve in (B) is fitted by a linear regression using all treatments in the experiment. At the prey concentrations of $<1 \times 10^7$ cells ml^{-1}, Ingestion rate (IR, cells $predator^{-1}$ d^{-1}) = 0.187 (pc × 10^6), $r^2 = 0.886$.

3.3.3. Growth and ingestion of K. japonica on bacterial prey

With increasing initial prey concentration, the ingestion rates of *K. japonica* on heterotrophic bacteria increased rapidly at prey concentrations of ca. 1.1–5.0 × 10^5 cells ml^{-1}, but slowly at the higher prey concentrations (Fig. 7A). When the data were fitted to Eq. (3), the maximum ingestion rate of *K. japonica* on heterotrophic bacteria was 266 bacteria $predator^{-1}d^{-1}$ (0.019 ng C $predator^{-1}d^{-1}$).

With increasing initial prey concentration, the ingestion rates of *K. japonica* on *Synechococcus* sp. increased continuously at prey concentrations of ca. 0.4–9.8 × 10^6 cells ml^{-1} (Fig. 7B). At the given prey concentrations, the highest ingestion rate of *K. japonica* on *Synechococcus* sp. was 48 *Synechococcus* $predator^{-1}d^{-1}$ (0.01 ng C $predator^{-1}d^{-1}$).

3.4. Discussion

3.4.1. Prey items and feeding behavior of Katablepharis japonica

This study revealed that *K. japonica* could feed on both bacterial and algal prey. Cells of *K. japonica* were revealed to feed on all tested algal prey species, except *Skeletonema costatum*, *Gambierdiscus caribaeus*, *Heterocapsa triquetra, Lingulodinium polyedra, Prorocentrum cordatum*, *P. micans, Alexandrium catenella*, and *Scrippsiella acuminata*. The range of the sizes of the edible prey species was wide; some prey species were

spherical, whereas others were flattened (e.g., *Prorocentrum donghaiense*); some prey species were singular, whereas others were chain-forming (*Cochlodinium polykrikoides* and *Gymnodinium catenatum*); some prey species were non-thecate, whereas others were thecate (*Heterocapsa rotundata, P. donghaiense*, and *Alexandrium minutum*). Thus, *K. japonica* has diverse prey items, regardless of sizes, shapes, toxicity, and presence of theca. Among phagotrophic protists, engulfment feeders usually feed on prey items that are smaller than themselves (Jeong et al., 2010b). The ability of *K. japonica* to feed on prey larger than itself is related to its feeding behavior; it engulfs small pieces of prey materials after causing the prey surface to rupture by pecking, however, the surface of *S. costatum*, *G. caribaeus*, *H. triquetra, L. polyedra, P. cordatum, P. micans, A. catenella*, and *S. acuminata* cells were not ruptured even though *K. japonica* cells pecked these algal cells many times for ≤48 h. Thus, these algal cells may have surfaces hard enough to resist dissolution by force or chemicals driven by *K. japonica*. Ecologically, *K. japonica* may not be abundant when *A. catenella*, *G. caribaeus*, *H. triquetra, L. polyedra, P. cordatum*, *P. micans, S. acuminata,* and *S. costatum* are abundant in natural environments.

Cells of *K. japonica* can feed on diverse phototrophic dinoflagellates. Furthermore, *K. japonica* grows well on *A. sanguinea* (previously *Gymnodinium splendens* and *G. sanguineum*), which has often formed red

tides or HABs in the coastal waters off many countries (Kiefer and Lasker, 1975; Jeong et al., 2013). This dinoflagellate is known to feed on small ciliates (Bockstahler and Coats, 1993). In the original microbial loop, a sequence of bacteria-HNFs-ciliates was suggested (Azam et al., 1983). Now, a new pathway in microbial food webs, bacteria-HNFs-ciliates-*A. sanguinea*-*K. japonica*, can be suggested. Cycling of materials among these components may be helpful for many species to co-exist. If there is no cycling in the food web, a predator may starve to death when its prey is eliminated by the predator.

Diverse red-tide dinoflagellates and raphidophytes are fed on by *K. japonica*. Grazing by heterotrophic dinoflagellates and/or ciliates is believed to contribute to the decline of red tides (Eppley and Harrison, 1975; Jeong, 1999; Kamiyama et al., 2000; Johnson et al., 2003; Kim and Jeong, 2004; Tillmann, 2004; Jeong et al., 2010b, 2015; Yoo et al., 2013), however, prior to the present study, the grazing effects by free-living HNFs like *Katablepharis* spp. on red tide species had not been explored, although there have been some studies on killing by parasitic heterotrophic flagellates on red tide species (e.g., Norén et al., 1999; Velo-Suárez et al., 2013; Alacid et al., 2015). The results of the present study suggest that grazing by free-living HNFs on red tide species should be taken into consideration in assessing red tide dynamics. Because of the addition of free-living HNFs as

grazers on red-tide organisms, total grazing effects by heterotrophic protistan grazers on populations of the red tide organisms are likely to increase.

Cells of *K. japonica* can feed on *Coolia malayensis,* which is a primarily benthic dinoflagellate (Ten-Hage et al., 2000; Penna et al., 2005; Fraga et al., 2008; Leaw et al., 2010; Laza-Martinez et al., 2011; Jeong et al., 2012a, 2012b), but not *G. caribaeus*, another benthic dinoflagellate. Instead, *G. caribaeus* immobilized *K. japonica* cells. Cells of *G. caribaeus* may have chemicals for anti-predation against *K. japonica*, which *C. malayensis* does not have. The size of *G. caribaeus* (ESD = 67.4 μm) is much larger than that of *C. malayensis* (ESD = 32.8 μm). Thus, a substantial difference in the sizes of these two benthic dinoflagellates might be partially responsible for the differential feeding of *K. japonica*. In turn, the differential feeding on these two benthic species may change the dominant species in the benthic dinoflagellate community.

Actively swimming *A. sanguinea* cells are fed on by *K. japonica* cells under both non-turbulent and turbulent conditions. Thus, *K. japonica* cells are likely to feed on actively swimming *A. sanguinea* cells in natural environments if the *K. japonica* concentration exceeds 100 cells ml^{-1}, however, *K. japonica* cells may feed on slow-moving or dead *A. sanguinea*

cells during the decline stage of *A. sanguinea* red tides or blooms, even when the *K. japonica* concentration is low.

3.4.2. Growth and ingestion rates

Prior to the present study, there were no reports on the growth rates of marine *Katablepharis* spp., whereas many reports on those of other HNFs exist (Table 8). Furthermore, there has been a report on a growth rate of a HNF on algal prey (Ohno et al., 2013). Therefore, this study adds useful information on growth rates of HNFs on algal prey.

Table 8

Comparison of the maximum growth and ingestion rates of *Katablepharis japonica* and other heterotrophic nanoflagellates. CV, cell volume (μm^3); CC, Carbon content per cell (ng C $cell^{-1}$); HTB, heterotrophic bacterial prey; MGR, maximum growth rate (d^{-1}); MIR, maximum ingestion rate (ng C $predator^{-1} d^{-1}$); CSMIR, carbon specific maximum ingestion rate (d^{-1}); MSS, maximum swimming speed ($\mu m\ s^{-1}$), blank, not tested.

Species name	CV	CC*	Prey	T	MGR	MIR	CS MIR	MSS	Ref
Monosiga sp.	20	0.004	HTB	20	4.080	0.070	19.4	25	(1)
Stephanoeca diplocostata	20	0.004	HTB	18	1.896	0.026	7.2		(2)
Ochromonas minima	25	0.004	HTB			-	-	75	(3)
Pseudobodo sp.	34	0.006	HTB	15	2.760	0.058	9.8		(4)
Codosiga gracilis	35	0.006	HTB	20	1.248	0.101	16.6		(5)
Diaphanoeca grandis	40	0.007	HTB	15	2.880	0.055	7.9	40	(6)
Ochromonas sp.	50	0.009	HTB	20	3.048	0.117	13.7		(7)

Pleuromonas jaculans	50	0.009	HTB	20	3.840	0.133	15.6		(1)
Bodo designis	54	0.009	HTB	20	3.840	0.437	47.8	80	(5)
Spurnella sp.	65	0.011	HTB	25	3.192	0.024	2.2		(8)
Pteridomonas danica	65	0.011	*Synechococcus* sp.	21	6.000		-		(9)
Pteridomonas danica	65	0.011	HTB	21	6.600		-		(9)
Actinomonas mirabilis	75	0.012	HTB	20	6.000	0.257	20.6	240	(1)
Jakoba libera	75	0.012	HTB	20	0.864	0.013	1.1	19	(5)
Stephanoeca diplocostata	83	0.014	HTB	20	0.840	0.099	7.2		(5)
Pseudobodo tremulans	90	0.015	HTB	20	3.600	0.199	13.4		(1)
Pyramimonas disomata	100	0.016	HTB				-	350	(3)

Paraphysomonas vestita	190	0.030	HTB	20	5.520	0.573	19.2	70	(1)
Ochromonas sp.	200	0.031	HTB	20	4.560	0.316	10.1	75	(1)
Paraphysomonas imperforata	212	0.033	HTB	20	5.040	0.159	4.8	42	(5)
Ciliophrys infusionum	220	0.034	HTB	20	1.080	0.649	19.0		(5)
Katablepharis japonica	278	0.043	*Akashiwo sanguinea*	20	1.010	0.132	2.2	530	(10)
Katablepharis japonica	278	0.043	HTB	20	0	0.015	0.2	530	(10)
Katablepharis japonica	278	0.043	*Synechococcus* sp.	20	0	0.010	0.2	530	(10)
Unidentified HNF	2590	0.347	*Skeletonema costatum*	15	0.790	0.660	1.2		(11)

(1) Fenchel (1982), (2) Geider and Leadbeater (1988), (3) Throndsen (1973), (4) Rivier et al. (1985), (5) Eccleston-Parry and Leadbeater (1994), (6) Andersen (1988), (7) Andersson et al. (1989), (8) Holen and Boraas (1991), (9) Zwirglmaier et al. (2009), (10) This study, (11) Ohno et al. (2013). CC*: Carbon content per cell was estimated from cell volume according to Menden-Deuer and Lessard (2000).

The maximum growth rate (μ_{max}) of *K. japonica* feeding on *A. sanguinea* (1.01 d^{-1}) is comparable to or slightly greater than that of *Jakoba libera*, *Stephunoeca diplocostuta*, and *Ciliophrys infusionurn* on bacteria (0.84–1.08 d^{-1}) or unidentified HNF on the diatom *Skeletonema costatum* (0.79 d^{-1}) (Geider and Leadbeater, 1988; Eccleston-Parry and Leadbeater, 1994; Ohno et al., 2013), however, the μ_{max} of *K. japonica* on *A. sanguinea* was lower than that of other reported HNF on bacteria (1.25–6.60 d^{-1}) (Table 8; Fig. 7A). In general, μ_{max} of HNFs decreases with increasing cell volume (Fenchel, 1987). Most HNFs reported are smaller than *K. japonica*. Thus, the larger size of *K. japonica* may be partially responsible for the lower μ_{max}. However, the μ_{max} of *K. japonica* feeding on *A. sanguinea* is much lower than that of *Paraphysomonas imperforata*, *Paraphysomonas vestita*, and *Ochromonas* sp., whose sizes are slightly smaller than *K. japonica*. The maximum ingestion rate (I_{max}) of *K. japonica* feeding on *A. sanguinea* is considerably lower than that of *P. imperforata*, *P. vestita*, and *Ochromonas* sp. on bacteria (Table 8; Fig. 7B). It may be more difficult for *K. japonica* to capture, ingest, and digest the dinoflagellate species (e.g., probably because of swimming speed, large-sized prey) than for *P. imperforata*, *P. vestita*, and *Ochromonas* sp. to capture, ingest, and digest bacterial prey. This lower I_{max} for *K. japonica* feeding on *A. sanguinea* may be partially responsible for the lower μ_{max}. Moreover, the carbon specific

maximum ingestion rate (CSI_{max}) of *K. japonica* feeding on *A. sanguinea* was lower than that of the HNFs, with exceptions of smaller *J. libera* and *Spurnella* sp. feeding on bacteria or unidentified HNF feeding on *S. costatum* (Table 8; Fig. 8C). Thus, the lower CSI_{max} of *K. japonica* feeding on *A. sanguinea* also may be partially responsible for this lower μ_{max} than that of most HNFs.

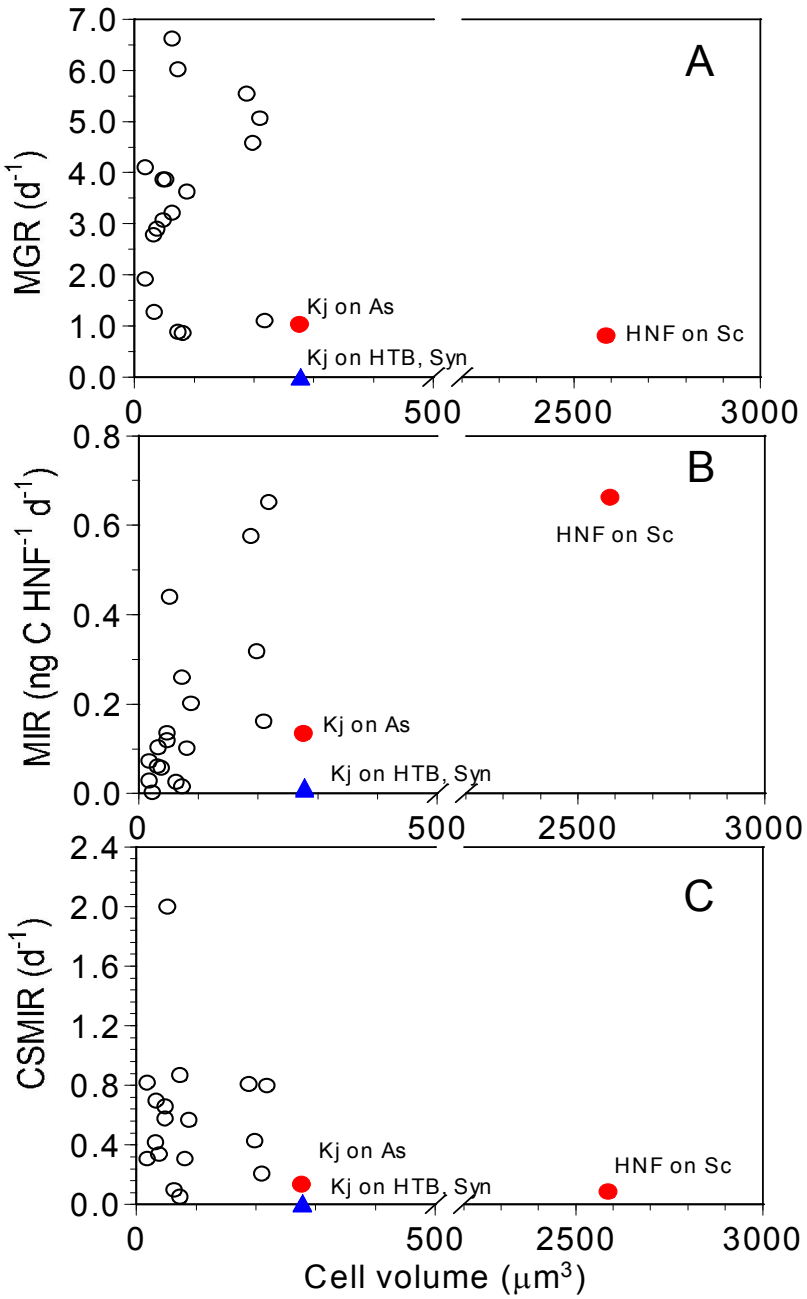

Fig. 8. Abundances of the red-tide dinoflagellate *Akashiwo sanguinea* (A) and heterotrophic nanoflagellates (HNFs, B) at a fixed station in Masan Bay from June 1, 2004 to May 31, 2005 (redrawn from Jeong et al. (2013) and Yoo et al. (2013), and (C) calculated grazing coefficients (g, d^{-1}) attributable to *Katablepharis japonica* on populations of *Akashiwo sanguinea* (see text for calculation).

Neither heterotrophic bacteria nor *Synechococcus* sp. supported positive growth of *K. japonica*. When combining maximum or highest ingestion rates and prey carbon, *K. japonica* can acquire 307% of its body carbon from *A. sanguinea*, but only 43 and 22% from heterotrophic bacteria and *Synechococcus* sp., respectively (Table 9). Therefore, low daily carbon acquisition from bacterial prey could be responsible for the lack of positive growth of *K. japonica*, whereas the high daily carbon acquisition from *A. sanguinea* prey supported substantial positive growth for *K. japonica*. To the best of my knowledge, *K. japonica* is the first reported HNF that can grow on algal prey, but not grow on bacteria prey. These results may change my conventional view on the critical role of bacteria as the optimal prey item to support growth of HNFs. An uncoupling between the abundance of *K. japonica* (or total HNFs if *K. japonica* is a dominant HNF) and bacteria in natural environments should be expected.

Table 9

Comparison of carbon acquisition of *Katablepharis japonica* (Kj) from *Akashiwo sanguinea*, heterotrophic bacteria (HTB), and the cyanobacterium *Synechococcus* sp. prey. PC, prey carbon (pg C per cell); MIR-cell, maximum ingestion rate (cells predator^{-1}d^{-1}); MIR-carbon (h), maximum ingestion rate (pg C predator^{-1}h^{-1}); MIR-carbon (d), maximum ingestion rate (pg C predator^{-1}d^{-1}); KjC, Kj carbon (pg C per cell); DAC, daily acquired carbon from prey relative to the predator carbon (%).

Prey	PC	MIR-cell	MIR-carbon (h)	MIR-carbon (d)	KjC	DAC
Akashiwo sanguinea	2230.00			132.0	43	307
HTB	0.07[&]	11.1	0.78	18.6	43	43
Synechococcus sp.	0.20[#]	2.0*	0.4*	9.5*	43	22

[&]: Simon and Azam (1989), recalculated by Norland (1993).

[#]: Jeong et al. (2005).

*: Highest value among all values obtained at a given concentration.

The results of the present study show that *K. japonica* is a predator of diverse phytoplankton, including toxic or harmful dinoflagellates and raphidophytes and may also affect dynamics of red tides caused by these prey species.

Chapter 4. The first report of the phototrophic dinoflagellate *Heterocapsa minima* in Korean waters and its interactions with common heterotrophic protists

4.1. Introduction

The dinoflagellate genus *Heterocapsa* is composed of small armored dinoflagellates, but the species in the genus are distributed worldwide in coastal waters. Some *Heterocapsa* species such as *Heterocapsa rotundata* (Lochmann) Hansen and *Heterocapsa triquetra* (Ehrenberg) F. Stein often form red tides causing shellfish mass mortalities (Matsuyama et al., 1995, Matsuyama 1999).

H. minima was first described by Pomroy (1989) based on samples collected in the Celtic Sea in 1982-1983. This species has been reported only from the European Ocean (Pomroy 1989; Salas et al. 2014). I isolated a small dinoflagellate from Mijo Port, Korea in 2016. Based on molecular analysis, this dinoflagellate was revealed to be *Heterocapsa minima*. *H. minima* formed dense blooms in Celtic Sea (ca. 62,400 cells l^{-1}) (Pomroy, 1989). Thus, there is a high possibility that this species causes harmful effects on marine organisms during or after dense blooms.

Heterotrophic protists are major microzooplankton and macrozooplankton, respectively, in marine ecosystems and play important

roles in marine food webs (Stoecker and Sanders, 1985; Sherr and Sherr, 1994, 2016; Jeong 1999; Calbet and Landry, 2004; Calbet et al., 2009; Yoo et al., 2013b, 2015; Lee et al., 2014; Turner, 2014; Petitpas et al., 2015; Jang et al., 2016). Heterotrophic protists such as heterotrophic dinoflagellates and ciliates have been revealed as effective grazers on many phototrophic dinoflagellates. Furthermore, the grazing impacts by heterotrophic protists on populations of phototrophic dinoflagellates are sometimes high enough to control prey populations. Therefore, mortality due to predation by heterotrophic protists should be studied to understand phototrophic dinoflagellate dynamics in marine ecosystems.

In addition, HTDs and ciliates are major components in marine ecosystems (Stoecker et al. 1984; Hansen 1991; Jeong 1999; Levinsen and Nielsen 2002; Sherr and Sherr 2007; Jeong et al. 2010b, 2015; Yoo et al. 2013a; Lim et al. 2017). They feed on diverse types of prey, such as bacteria, phytoplankton including red-tide species, mixotrophic, or heterotrophic protists, eggs and early naupliar stages of metazooplankton, and sometimes control populations of their prey (Hansen 1992; Jeong 1994; Montagnes et al. 1996; Jeong et al. 2004, 2008; Kamiyama and Matsuyama 2005; Turner 2006; Yoo et al. 2013b; Lee et al. 2014; Jang et al. 2016; Lim et al. 2017). In general, due to much higher abundances of HTDs or ciliates than those of metazooplankton, effect of grazing on prey populations by the former

grazers is usually greater than that by the latter grazers (Kim et al. 2013, Yoo et al. 2013a). Thus, to understand the roles of potential prey species in food webs, feeding by HTDs or ciliates on the prey should be explored. Therefore, I investigated whether *H. minima* attacks common heterotrophic protists or not. The results of the present study provide a basis for understanding the interactions between *H. minima* and common heterotrophic protist species, and their ecological roles in the marine planktonic community. To the best of my knowledge, no studies have been reported on the protist predators of *H. minima*. To understand the roles of *H. minima* in red tide dynamics, mortality due to predation should be determined.

For better understanding of the ecology of *H. minima* in marine ecosystems, further studies on of the interactions between *H. minima* and common predatory plankton are required. Therefore, in the present study, genetic characterization of the phototrophic dinoflagellate *H. minima* and feeding behaviors of the common heterotrophic protists on *H. minima* and vice versa were observed. The results of the present study provide a basis on understanding the interactions between *H. minima* and common heterotrophic protists, and their ecological roles in the marine planktonic community.

4.2. Materials and Methods

4.2.1. Sequencing and phylogenetic analysis

DNA sequencing

Three to five cells of *H. minima* from a clonal culture were transferred to a 0.2-ml PCR tube containing 38.75 µl of distilled water. To break the cell membranes before PCR analysis, the tube was frozen at −72°C for 1–3 min and then thawed. The final mixture (50 µl total volumes) was vortexed and PCR reaction was performed as follows: A thermal cycler (Eppendorf AG, Mastercycler® ep, model 5341, Hamburg, Germany) was used for the PCR reactions. The final concentrations of PCR products were: 5 µl of 10X F-StarTaq buffer, 1 µl of 10 mM of dNTP mix, 0.25 µl of 5 U/µl BioFACT™ F-Star Taq DNA polymerase (BioFACT Co., Ltd., Daejeon, Korea), 0.02 µM of each primer, for a final volume of 50 µl. The following primer pairs were used for amplification of ITS region, and LSU (D1-D2) rDNA sequences: ITSF2 (5′ - TAC GTC CCT GCC CTT TGT AC -3′ ; Litaker et al. 2003) and ITSR2 (5′ - TCC CTG TTC ATT CGC CAT TAC -3′ ; Litaker et al. 2003); and D1RF (5′ - ACC CGC TGA ATT TAA GCA -3′ ; Scholin et al. 1994), and LSUB (5′ - ACG AAC GAT TTG CAC GTC AG -3′ ; Litaker et al. 2003). The PCR conditions were as follows: one activation step at 95°C for 2 min; followed by 35 cycles at 95°C for 20 s, the selected annealing temperature (AT) for 40 s, and 72°C

for 1 min; a final elongation step at 72°C for 5 min. The AT was adjusted depending on the primers used according to the manufacturer's instructions.

Positive and negative controls were used for all amplification reactions. The purity of the amplicons was checked by electrophoretically separating 3-μl of PCR products mixed with 0.5-μl of goRed fluorescent reagent using a 1.0% agarose gel at 100 V and observing it under a UV lamp to ensure that a single product was formed. Products containing a single band were then purified using an AccuPrep® PCR purification kit (Bioneer Corp., Daejeon, Korea) according to the manufacturer's instructions. The purified DNA was sent to the Genome Research Facility at School of Biological Science, Seoul National University, Korea, and sequenced with an ABI PRISM® 3700 DNA Analyzer (Applied Biosystems, Foster City, CA, USA). Each portion of the target DNA was independently sequenced three times in both directions using primer pairs identical to those used for DNA amplification. Sequences were aligned using the ContigExpress alignment program (InforMax, Frederick, MD, USA) to edit out low-quality regions and to assemble the individual sequence reads.

Phylogenetic analyses

Separate phylogenetic analyses were performed based on alignments of partial 3′ end ITS and LSU (full sequence of the domain D1–D2) sequences. Analyses included sequences obtained from GenBank.

Multiple sequences were aligned automatically using MEGA4´ s native implementation of ClustalW (Tamura et al. 2007), then further aligned manually by eye for refinement of the alignments. Maximum-likelihood (ML) analyses were performed using the RAxML 7.0.3 program (Stamatakis 2006) with default GTR + G model. Tree likelihoods were estimated using a heuristic search with 100 random additional sequence replicates and tree bisection and reconnection branch swapping. ML bootstrapping with 1,000 replications was also conducted. Bayesian analyses were performed using MrBayes v.3.1 (Huelsenbeck and Ronquist 2001; Ronquist and Huelsenbeck 2003) with the GTR + G model to determine the best available model for the data for each region. Phylogenetic trees were created for all sequences using four independent Markov Chain Monte Carlo runs performed simultaneously until average standard deviation of split frequencies dropped below 0.01. The trees were sampled every 1,000 generations. To ensure likelihood convergence, the first 800 trees were discarded as burn-in.

4.2.2. Preparation of experimental organisms

A clonal culture of *H. minima*, which was isolated from plankton samples collected from Mijo Port, Korea in April 2016. As the concentration of *H. minima* increased, the culture was transferred to 250-ml

flasks (approximately 200,000 cells ml^{-1}). The flasks were filled to capacity with freshly filtered seawater, capped, and placed on a shelf at 20°C under an illumination of 20 μE m^{-2} s^{-1} provided by cool white fluorescent lights, under a 14 : 10 h light : dark cycle. The mean equivalent spherical diameter (± standard deviation) and carbon content of *H. minima* were 8.2 μm (± 0.2) and 0.04 ng C per cell, respectively.

For the isolation and culture of the HTD predators *Gyrodinium dominans*, *Oblea rotunda*, *Oxyrrhis marina*, and *Polykrikos kofoidii*, plankton samples were collected by using water samplers, from the coastal waters off Jangheung, Jinhae, or Shiwha, Korea during 2008–2016 (Table 9). A clonal culture of each species was established by using two serial single-cell isolations (Table 10). A clonal culture of *Pfiesteria pisicicida* was obtained from Microbiota, United States.

Table 10

Isolation and maintenance conditions for the experimental organisms

Organism	Location	Time	T	S	FM	Prey species
Heterotrophic dinoflagellate						
Gyrodinium dominans	Shiwha Bay, Korea	Nov 2011	19.7	31.0	EG	*Amphidinium carterae*
Oblea rotunda	Jinhae Bay, Korea	Apr 2015	12.6	31.2	PA	*Amphidinium carterae*
Oxyrrhis marina	Shiwha Bay, Korea	Dec 2008	16.8	27.0	EG	*Amphidinium carterae*
Polykrikos kofoidii	Jangheung Bay, Korea	Jul 2016	23.6	26.4	EG	*Scrippsiella trochoidea*
Pfiesteria piscicida (CCMP2091)	Neuse River, USA	Jan 1998	-	-	PE	*Amphidinium carterae*
Ciliate						
Pelagostrobilidium sp.	Tongyoung, Korea	Aug 2017	27.2	31.5	EG	*Prorocentrum minimum*

Sampling location and time; water temperature (T, °C), salinity (S) for isolation; feeding mechanisms (FM), and prey species.

EG, engulfment feeder; PE, peduncle feeder; PA, pallium feeder.

For the isolation and culture of the ciliate *Pelagostrobilidium* sp. (approximate cell length = 50 μm), plankton samples were collected by using a 10-μm mesh, in coastal waters off Tongyoung, Korea in August 2017 when the water temperature and salinity were 27.2°C and 31.5, respectively (Table 10).

The carbon contents of the HTDs and the ciliate were estimated from the cell volume, according to the procedure of Menden-Deuer and Lessard (2000). The cell volumes of the predators were estimated using the methods of Kim and Jeong (2004) and Yoon et al. (2012) for *G. dominans*, that of Jeong et al. (2008) for *O. marina*, Jeong et al. (2001) for *P. kofoidii*, Jeong et al. (2007) for *P. piscicida*, and Kim et al. (2017) for *O. rotunda*, and *Pelagostrobilidium* sp. (Table 10).

4.2.3. Interactions between Heterocapsa minima and heterotrophic protists

Experiment (Exp.) 1 was designed to investigate interactions between *H. minima* and each of the heterotrophic protists after two components was mixed (Table 11). In this experiment, it was tested whether the target heterotrophic protist is able to feed on *H. minima* and vice versa.

A culture of approximately 200,000 cells ml^{-1} of *H. minima* was transferred to a single 250-ml culture flask containing freshly filtered seawater. This culture was maintained for 1 day. Three 1-ml aliquots were

examined with a light microscope to determine the concentration of *H. minima*.

Table 11

Experimental design

Exp. No.	Species	Prey density	Species	Predator density
1	*Heterocapsa minima*	10,000	*Gyrodinium dominans*	4,000
		10,000	*Oblea rotunda*	2,000
		10,000	*Oxyrrhis marina*	4,000
		10,000	*Polykrikos kofoidii*	200
		10,000	*Pfiesteria piscicida*	5,000
		8,000	*Pelagostrobilidium* sp.	500
2	*Heterocapsa minima*	199, 484, 1,002, 2,075, 4,789, 9,296, 12,889, 20,863, 33,630, 51,222	*Gyrodinium dominans*	27, 68, 143, 250, 483 (547), 734, 967, 1,215, 1,450, 2,381 (2,406)

The numbers in the prey and predator columns are the target initial densities (cells ml^{-1}) of prey and predator for Exp. 1, and the actual initial densities for Exp. 2. The values within parentheses in the predator column in Exp. 2 are the predator densities in the control bottles.

The initial concentrations of *H. minima* (approximately 8,000–10,000 cells ml^{-1}) and each of the target heterotrophic protist species were established using an autopipette to deliver a predetermined volume of culture with a known cell density into the wells of 6-well plate chambers. For each heterotrophic protist species, duplicate wells containing mixtures of *H. minima* and heterotrophic protist (a total of 5-ml in each well), duplicate predator control wells containing a culture of heterotrophic protists only (a total of 5 ml in each well), and duplicate prey control wells containing a culture of *H. minima* only (a total of 5 ml in each well) were established. The plate chambers were placed on a shelf and incubated under a 14 : 10 h light : dark cycle of 20 μE m^{-2} s^{-1} of cool white fluorescent light.

After 2 and 24 h, >30 target predator cells in the well was monitored using an inverted epifluorescence microscope equipped with differential interference contrast at a magnification of 50–200× to determine whether the target predator species is able to feed on *H. minima* or not. The feeding process of each of these heterotrophic protists on *H. minima* was recorded using a video analyzing system (Sony DXC-C33; Sony Co., Tokyo, Japan) and also captured using a digital camera. The reciprocal feeding of *H. minima* on each of the heterotrophic protists was tested and recorded in the same manners as described above.

4.2.4. Effects of the Heterocapsa minima concentration on the growth rate of Gyrodinium dominans

In Exp. 1, *H. minima* fed on *G. dominans*. Thus, Exp. 2 was designed to measure the growth rate of *G. dominans* as a function of *H. minima* concentration (Table 11).

For the experiment *H. minima* were transferred to a single 250-ml culture flask containing freshly filtered seawater. This culture was maintained for 1 day. Three 1-ml aliquots were then collected from the flask and examined using a light microscope to determine the concentration of *H. minima*.

The initial concentrations of *H. minima* were established using an autopipette to deliver predetermined volumes of known cell concentrations to the flasks. For each predator-prey combination, triplicate 42-ml experimental flasks (containing a mixture of *H. minima* and predator) and triplicate control flasks (containing a culture of *H. minima* only) were established. Five milliliters of f/2-Si medium was added to all flasks, which were then filled to capacity with freshly-filtered seawater and capped, and then placed on a shelf at 20°C under a 14 : 10 h light : dark cycle of 20 μE m^{-2} s^{-1} of cool white fluorescent light. To determine the actual initial predator and prey densities (cells ml^{-1}) at the beginning of the experiment (Table 11) and after a 2-day incubation period, 10-ml aliquots were removed

from each flask and fixed with 5% Lugol's solution. Then, all *H. minima* cells and all or >300 prey cells in three 1-ml Sedgwick-Rafter chambers were enumerated.

The specific growth rate of *G. dominans* was calculated as follows:

$$\mu = \frac{\text{Ln}\,(C_t / C_0)}{t} \qquad (1)$$

where C_0 is the initial concentration of predator and C_t is the final concentration after time t. The period was 2 days. The mean prey concentration was calculated using the equation of Frost (1972). The ingestion and clearance rates were calculated using the equations of Frost (1972) and Heinbokel (1978).

4.2.5. Artemia test for toxicity

A bioassay using the brine shrimp *Artemia salina*, which is susceptible to saxitoxin (STX) was conducted. Encysted eggs of *A. salina* were hatched in 500-ml of filtrated natural seawater under artificial light at 20 °C for 48 h. Six-well plate chambers were prepared with triplicate wells of 100,1000, 5000, 10000, 30000, and 60000 cells ml^{-1} of *H. minima*, respectively, and then 10 *A. salina* nauplii were placed in each well of the plate chambers. In addition, triplicate wells containing a mixture of 10 nauplii and *H. minima*-filtrate as well as triplicate wells containing 10

nauplii only were established. The filtrate was obtained through filtration (grade GF/C) of a dense *H. minima* culture. As a positive control, *A. minutum* was used in an identical experimental setup. The plate chambers were incubated at 20 °C under a 14:10 h light–dark cycle of cool white fluorescent lights at 20 μE m^{-2} s^{-1}. At the beginning of the incubation and 1, 2, 4, 8, 12, 24, and 48 h later, the plate chambers were placed under a dissecting microscope, and living and dead nauplii were counted at a magnification of ×7–40.

4.3. Results

4.3.1. Phylogeny

The assumed equal nucleotide frequencies of ITS rDNA comprised a substitution rate matrix with A-C substitutions = 0.0771, A-G substitutions = 0.3129, A-T substitutions = 0.1071, C-G substitutions = 0.0198, C-T substitutions = 0.4348, and G-T substitutions = 0.0483. The proportion of sites assumed to be invariable was 0.1939 and the rates for variable sites were assumed to follow a gamma distribution with a shape parameter of 0.7881. The assumed equal nucleotide frequencies of LSU rDNA comprised a substitution rate matrix with A-C substitutions = 0.0511, A-G substitutions = 0.1556, A-T substitutions = 0.0971, C-G substitutions = 0.0624, C-T substitutions = 0.5361, and G-T substitutions = 0.0977. The proportion of

sites assumed to be invariable was 0.4867 and the rates for variable sites were assumed to follow a gamma distribution with shape parameter of 0.5657.

In the phylogenetic analyses based on the ITS and LSU (D1–D2) rDNA, *H. minima* was clearly divergent from the other clades (Figs. 9, 10).

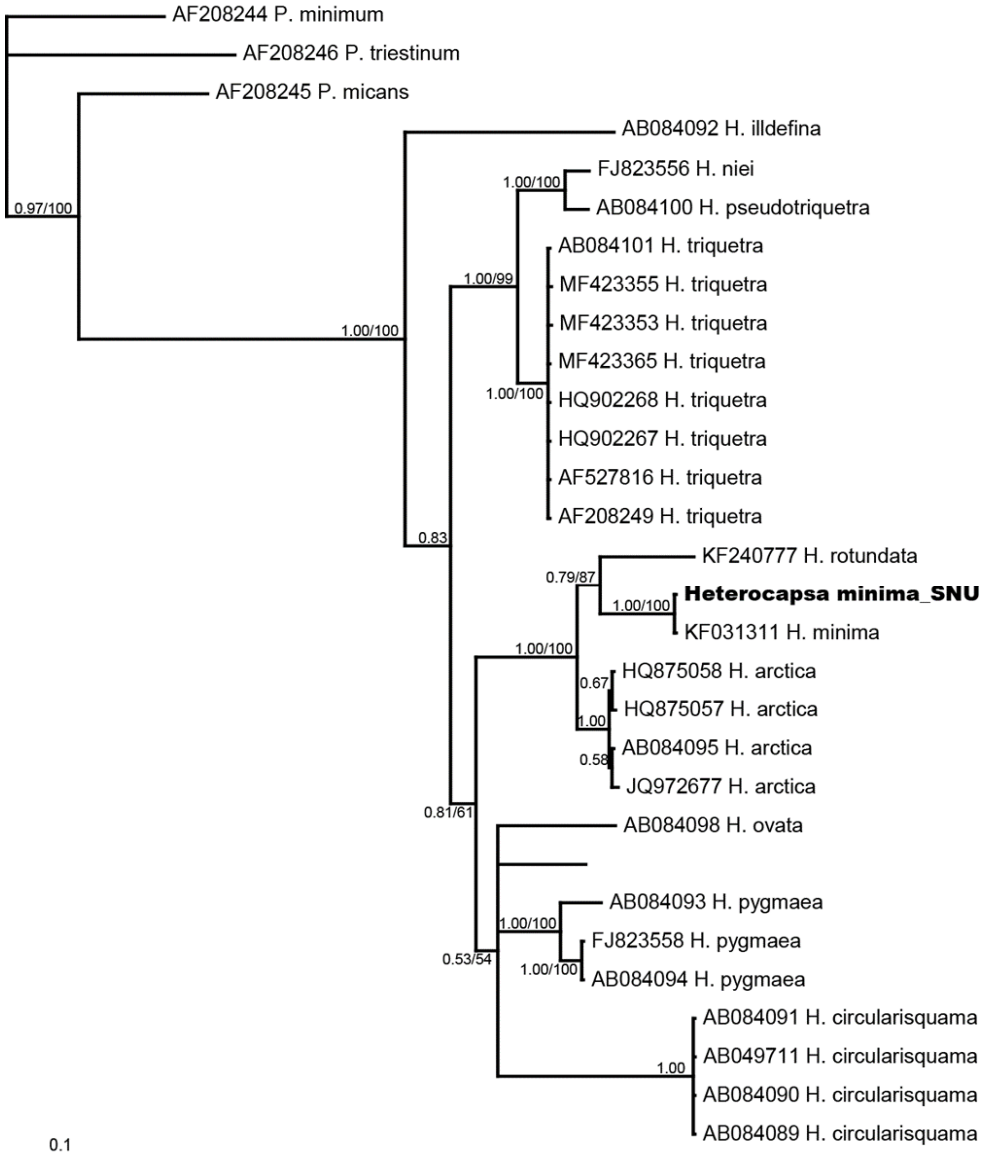

Fig. 9. Consensus Bayesian tree of the family Suessiaceae based on 767 aligned positions of ITS rDNA. *Prorocentrum* spp. were chosen as the outgroup taxon. The branch lengths are proportional to the amount of character change. The numbers above the branches indicate the Bayesian posterior probability (left) and maximum-likelihood bootstrap values (right).

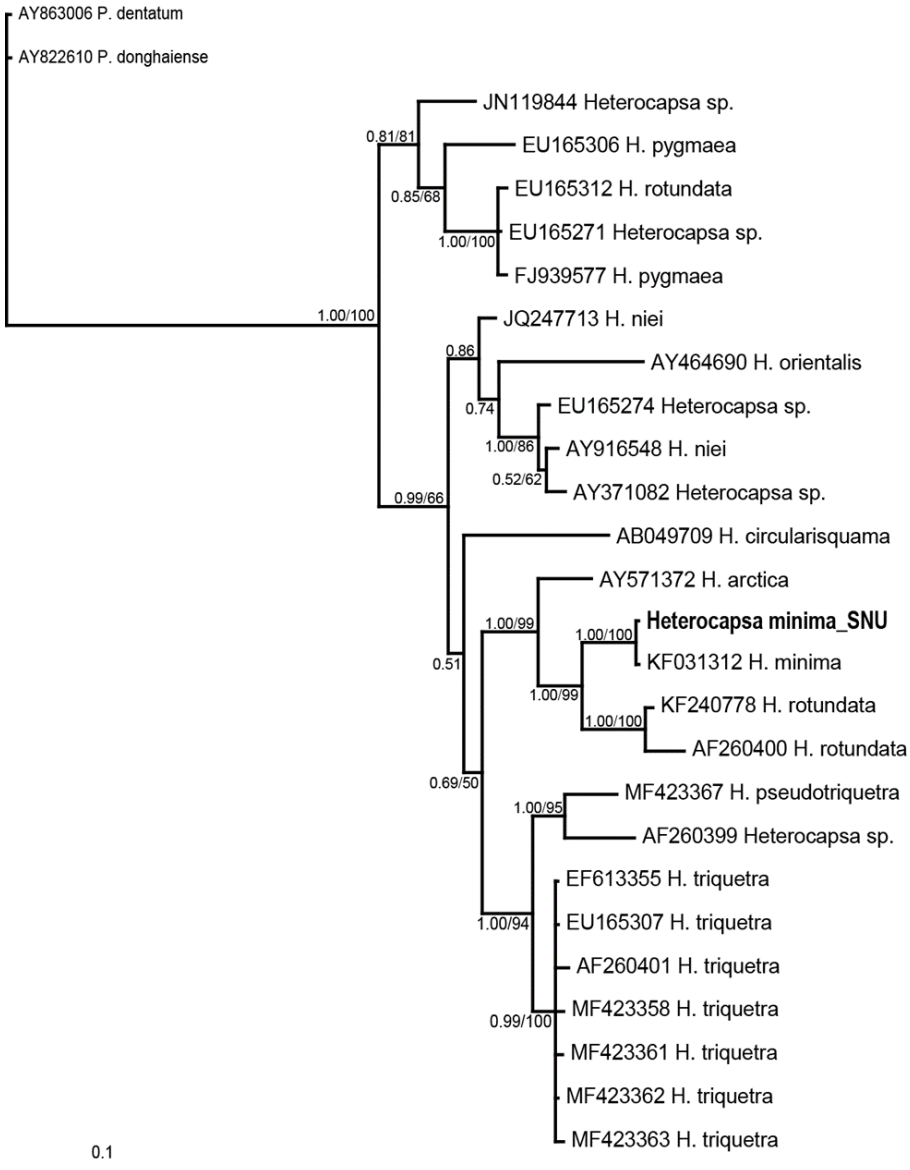

Fig. 10. Consensus Bayesian tree of the family Suessiaceae based on 889 aligned positions of LSU (D1-D2) rDNA. *Prorocentrum* spp. were chosen as the outgroup taxon. The branch lengths are proportional to the amount of character change. The numbers above the branches indicate the Bayesian posterior probability (left) and maximum-likelihood bootstrap values (right).

4.3.2. Interactions between *Heterocapsa minima* and common heterotrophic protists

Among the 6 common predator species tested in this study, Cells of *Oxyrrhis marina*, *Gyrodinium dominans*, *Pfiesteria piscicida*, and *Pelagostrobilidium* sp. were able to feed on *Heterocapsa minima* cells, but cells of *Oblea rotunda*, and *Polykrikos kofoidii* were not feed on *H. minima* (Table 12). *H. minima* were attacked by *O. rotundata*, but not eaten. Cells of *O. marina* and *G. dominans* contained 1–3 ingested prey cells.

Table 12

Taxa and size of common heterotrophic dinoflagellate and naked ciliate predators offered to *Heterocapsa minima*

Predators	ESD (µm)	Feeding of *H. minima*
Gyrodinium dominans	20.0	Y
Oblea rotunda	21.6	N
Oxyrrhis marina	15.6	Y
Polykrikos kofoidii	43.5	N
Pfiesteria piscicida	13.5	Y
Pelagostrobilidium sp.	42.4	Y

The initial concentrations of *H. minima* were 8,000–10,000 cells ml^{-1}. Mean equivalent spherical diameter (ESD, µm).

Y, feeding; N, no feeding.

Feeding by cells of *O. marina* on *H. minima* was confirmed by observation using epifluorescence microscopy (Fig. 11E). The body of *H. minima*, having chloroplasts, was seen as a red sphere under an epifluorescence microscope, while the body of *O. marina* was not seen because it does not have chloroplasts. The two species (predator and prey) were mixed, red particles were transferred from the bodies of *H. minima* to those of *O. marina*.

Feeding by cells of *G. dominans* on *H. minima* was confirmed by observation using epifluorescence microscopy (Fig. 11G). One *H. minima* cell inside the protoplasm of a *G. dominans* cell observed under an epifluorescence microscope.

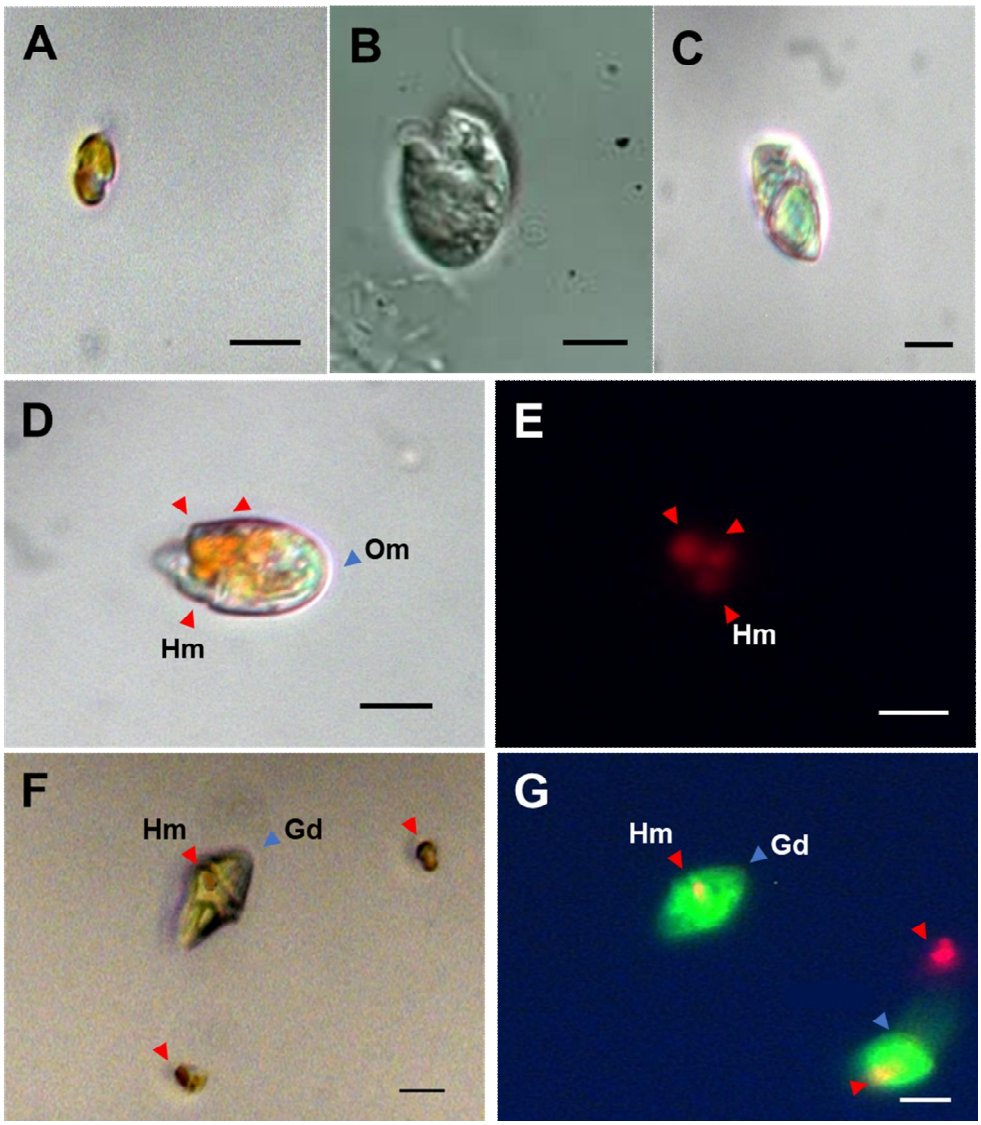

Fig. 11. Images of heterotrophic dinoflagellates feeding on *Heterocapsa minima* (Hm). *H. minima* cell without added predator observed under a light microscope (A), *Oxyrrhis marina* (Om) cell without added prey (B), and *Gyrodinium dominans* (Gd) cell without added prey (C), Feeding of Om cell (blue arrow) on Hm cells (red arrow) observed under an epifluorescence microscope without filters (D) or under green filter (E), Feeding of Gd cell (blue arrow) on Hm cell (red arrow) observed under an epifluorescence microscope without filters (F) or under green filter (G). Scale bar = 10 μm for (A-G).

4.3.3. Effects of the Heterocapsa minima concentration on the growth rate of Gyrodinium dominans

The growth rates of *O. marina*, *G. dominans*, *P. piscicida*, and *Pelagostrobilidium* sp. on *H. minima* were very low or negative at almost all prey concentrations. The specific growth rate of *G. dominans* on *H. minima* at the all prey concentration (8-2049 ng C ml^{-1}) (range = -0.25 d^{-1} ~ -0.14 d^{-1}) was lower than that of *G. dominans* without added prey (mean ± standard error = 0.034 d^{-1} ± 0.017, n = 3) ($p > 0.1$, two-tailed *t*-test). The specific growth rate of *G. dominans* incubated with *H. minima* was significantly lower than that without *H. minima* (Fig. 12).

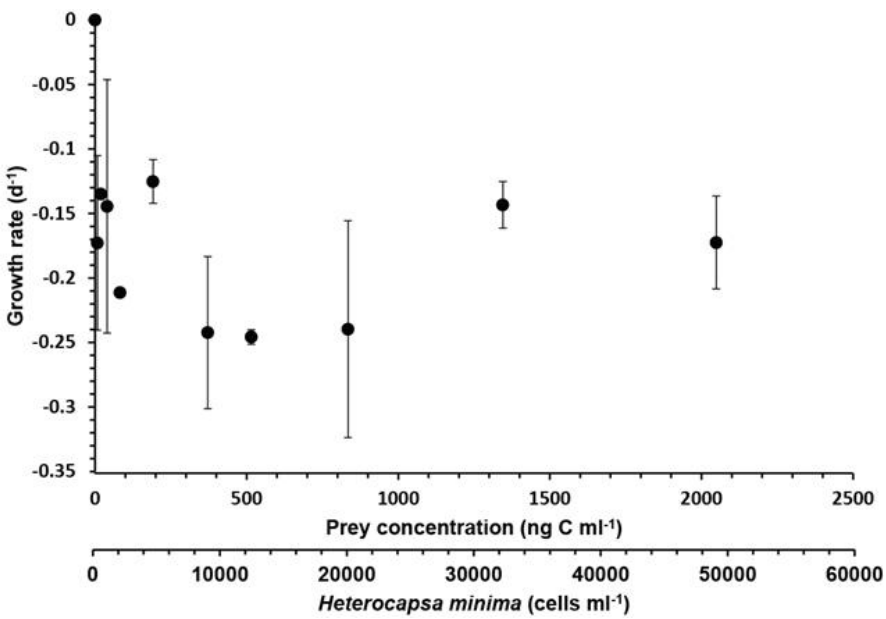

Fig. 12. Growth rates of *Gyrodinium dominans* on *Heterocapsa minima* as a function of mean prey concentration.

4.3.4. Artemia test for toxicity

One to two (average = 1.7) of 10 *Artemia salina* nauplii in each well died after 48 h incubation with *A. minutum* at the concentrations of >1000 cells ml^{-1}, while almost all nauplii survived after incubation with *A. minutum* filtrate. However, almost all nauplii of *A. salina* survived after 48 h of incubation with *H. minima* (>100 cells ml^{-1}), but two to three *A. salina* nauplii per well aggregated and thus could not swim normally. None of the *A. salina* nauplii was dead after 48 h of incubation with *H. minima* filtrate.

4.4. Discussion

4.4.1. Interactions between Heterocapsa minima and common heterotrophic protists

This study clearly showed that common HTDs and ciliates fed on *H. minima.* Of the HTDs included in the present study, *O. marina*, *G. dominans*, *Pelagostrobilidium* sp. and *P. piscicida* fed on *H. minima* cells, whereas *O. rotunda*, *P. kofoidii* did not feed on *H. minima*. The HTDs *O. rotunda*, and *P. kofoidii* attempt to feed on *H. minima* cells. *O. rotunda* uses a tow filament, and *P. kofoidii* uses a nematocyst-taeniocyst complex (Strom and Buskey 1993; Kiφrboe and Titelman 1998; Matsuoka et al. 2000; Jeong et al. 2001). Therefore, *H. minima* cells may not draw deployment of a tow filament or a nematocyst-taeniocyst complex.

4.4.2. Effects of the Heterocapsa minima concentration on the growth rate of Gyrodinium dominans

When suitable prey species are provided, the specific growth rates of *G. dominans* were negative at almost all prey concentrations. The phototrophic dinoflagellate prey *Prorocentrum minimum*, *Heterocapsa triquetra*, and the raphidophyte *Chattonella antiqua* cause this positive trend (Kim et al., 2004; Nakamura et al., 1995; Nakamura et al., 1992). When *G. dominans* fed on *H. triquetra*, the maximum growth rate of *G. dominans* was 0.54 d^{-1}. However, in the present study, the specific growth rate of *G. dominans* was very low or negative at almost all prey concentrations. Thus, *H. minima* may neither markedly support nor inhibit the growth of *G. dominans.*

4.4.3. Ecological niche

Interestingly, the results of this study show that, while *A. minutum* cells kill *Artemia salina* nauplii, *H. minima* cells do not. *H. minima* may not have harmful ingredients for the predators and may not affect growth of predators. This study shows that *H.minima* is not a good prey for predators. When *Heterocapsa* spp. bloom occurs, predators are expected to eat other species that can grow through eating instead of the innutritious *H. minima.* Thus, *H. minima* might play diverse ecological roles in marine planktonic

communities by having an advantage over competing phytoplankton in anti-predation against common protistan grazers.

Chapter 5. General conclusions

In this thesis, I explored the distribution of the heterotrophic nanoflagellate *Katablepharis japonica* in Jinhae Bay from May 2014 to July 2017. Furthermore, I discovered a newly identified role of *K. japonica*, an effective predator on red-tide organisms. Moreover, I first reported the presence of the phototrophic dinoflagellate *Heterocapsa minima* in Korean waters and investigated its interactions with common heterotrophic protists.

From the data on the abundance of *Katablepharis japonica* in Jinhae Bay, Korea from May 2014 to July 2017, quantified using qPCR method and newly designed specific primer-probe sets, the abundances of *K. japonica* was affected by chlorophyll-a concentration. This evidence suggests that this HNF may feed on phytoplankton. The subsequent feeding experiments showed that *K. japonica* is a predator of diverse phytoplankton, including toxic or harmful dinoflagellates and raphidophytes. Prior to this study, most protistan predators on toxic or harmful dinoflagellates and raphidophytes were mixotrophic dinoflagellates, heterotrophic dinoflagellates, and ciliates. However, this discovery extends protistan predators to HNFs. Furthermore, mortality due to predation by HNFs should be taken into consideration in establishing models of understanding or predicting process of red tides or harmful algal blooms.

Prior to this study, *Heterocapsa minima* was reported only from the European Ocean. Discovery of this species in the Korean waters extends its distribution to the Pacific Ocean. Using a clonal culture of this species, interactions between this species and common heterotrophic protistan predators were explored. The heterotrophic dinoflagellates *Oxyrrhis marina, Gyrodinium dominans,* and *Pfiesteria piscicida* and the naked ciliate *Pelagostrobilidium* sp. fed on *Heterocapsa minima* cells, whereas the heterotrophic dinoflagellates *Oblea rotunda* and *Polykrikos kofoidii* did not feed on *H. minima* cells. However, the specific growth rates of predators were very low or negative at almost all prey concentrations. Thus, *H. minima* did not support growth of all common heterotrophic protists tested. Furthermore, its mortality due to predation by heterotrophic protistan predators may be very low.

References

Alacid, E., Reñé, A., Garcés, E., 2015. New insights into the parasitoid *Parvilucifera sinerae* life cycle: the development and kinetics of infection of a bloom-forming dinoflagellate host. Protist, 166 (6), 677-699.

Andersen, P., 1988. Functional biology of the choanoflagellate *Diaphanoeca grandis* Ellis. Mar. Microb. Food Webs 3 (2), 35-49.

Anderson, D.M., 1989. Toxic algal blooms and red tides: a global perspective. In: Okaichi, T., Anderson, D.M., Nemoto, T. (Eds.), Red tides: Biology, environmental science and toxicology. Elservier, New York, pp. 11-16.

Andersson, A., Falk, S., Samuelsson, G., Hagström, Å., 1989. Nutritional characteristics of a mixotrophic nanoflagellate, *Ochromonas* sp. Microb. Ecol. 17 (3), 251-262.

Antonella, P., Luca, G., 2013. The quantitative real-time PCR applications in the monitoring of marine harmful algal bloom (HAB) species. Environ. Sci. Pollut. Res. 20 (10), 6851-6862.

Azam, F., Fenchel, T., Field, J.G., Gray, J.S., Meyer-Reil, L.A., Thingstad, F., 1983. The ecological role of water-column microbes in the sea. Mar. Ecol. Prog. Ser. 10, 257-263.

Basti, L., Nagai, K., Go, J., Okano, S., Oda, T., Tanaka, Y., Nagai, S., 2016. Lethal effects of ichthyotoxic raphidophytes, *Chattonella marina*, *C. antiqua*, and *Heterosigma akashiwo*, on post-embryonic stages of the Japanese pearl oyster, *Pinctada fucata martensii*. Harmful Algae 59, 112-122.

Berge, T., Poulsen, L.K., Moldrup, M., Daugbjerg, N., Hansen, P.J., 2012. Marine microalgae attack and feed on metazoans. The ISME journal 6 (10), 1926.

Bockstahler, K.R., Coats, D.W., 1993. Grazing of the mixotrophic dinoflagellate *Gymnodinium sanguineum* on ciliate population of Chesapeake Bay. Mar. Biol. 116, 447-487.

Calbet, A., Landry, M.R., 2004. Microzooplankton production in the oceans. ICES J. Mar. Sci. 61 (4), 501-507.

Calbet, A., Atienza, D., Henriksen, C.I., Saiz, E., Adey, T.R., 2009. Zooplankton grazing in the Atlantic Ocean: A latitudinal study. Deep Sea Research Part II: Topical Studies in Oceanography, 56 (15), 954-963.

Clay, B., Kugrens, P., 1999. Systematics of the enigmatic kathablepharids, including EM characterization of the type species, *Kathablepharis phoenikoston*, and new observations on *K. remigera* comb. nov. Protist 150 (1), 43-59.

Deeds, J.R., Landsberg, J.H., Etheridge, S.M., Pitcher, G.C., Longan, S.W., 2008. Non-traditional vectors for paralytic shellfish poisoning. Marine Drugs 6 (2), 308-348.

Dodge, J.D., 1971. A dinoflagellate with both a mesocaryotic and a eucaryotic nucleus I. Fine structure of the nuclei. Protoplasma 73 (2), 145-157.

Dodge, J.D., 1975. A survey of chloroplast ultrastructure in the Dinophyceae. Phycologia 14 (4), 253-263.

Eccleston-Parry, J.D., Leadbeater, B.S., 1994. A comparison of the growth kinetics of six marine heterotrophic nanoflagellates fed with one bacterial species. Mar. Ecol. Prog. Ser. 105, 167-177.

Eppley, R.W., Harrison, W.G., 1975. Physiological ecology of *Gonyaulax polyedrum*, a red tide water dinoflagellate of southern California. In: Locicero, V.R. (Ed.) Preceedings First International Conference on Toxic Dinoflagellate Blooms. Massachusetts Science and Technology Foundation. Wakefield, Massachusetts, p. 11-22.

Fenchel, T., 1982. Ecology of heterotrophic microflagellates. 11. Bioenergetics and growth. Mar. Ecol. Prog. Ser. 8, 225-231.

Fenchel, T., 1987. Ecology of protozoa. Springer, Berlin, pp. 197.

Fraga, S., Penna, A., Bianconi, I., Paz, B., Zapata, M., 2008. *Coolia canariensis* sp. nov. (Dinophyceae), a new nontoxic epiphytic benthic dinoflagellate from the Canary Islands. J. Phycol. 44 (4), 1060-1070.

Frost, B.W., 1972. Effects of size and concentration of food particles on the feeding behavior of the marine planktonic copepod *Calanus pacificus*. Limnol. Oceanogr. 17, 805-815.

Garson, G.D., 2013. Factor analysis. Statistical Associates.

Geider, R.J., Leadbeater, B.S., 1988. Kinetics and energetics of growth of the marine choanoflagellate *Stephanoeca diplocostata*. Mar. Ecol. Prog. Ser. 169-177.

Gibbs, S.P., 1981. The chloroplasts of some algal groups may have evolved from endosymbiotic eukaryotic algae. Ann. NY Acad. Sci. 361 (1), 193-208.

Grattan, L.M., Holobaugh, S., Morris, J.G., 2016. Harmful algal blooms and public health. Harmful algae 57, 2-8.

Guillard, R.R.L., Ryther, J.H., 1962. Studies of marine planktonic diatoms. I. *Cyclotella nana* Hustedt and *Detonula confervacea* (Cleve) Grun. Can. J. Microbiol. 8, 229-239.

Hallegraeff, G.M., 1993. A review of harmful algal blooms and their apparent global increase. Phycologia 32 (2), 79-99.

Hansen, P.J., 1991. Quantitative importance and trophic role of heterotrophic dinoflagellates in a coastal pelagial food web. Mar. Ecol. Prog. Ser. 73 (2-3), 253-261.

Hansen, P.J., 1992. Prey size selection, feeding rates and growth dynamics of heterotrophic dinoflagellates with special emphasis on *Gyrodinium spirale*. Mar. Biol. 114 (2), 327-334.

Hansen, P.J., 2011. The role of photosynthesis and food uptake for the growth of marine mixotrophic dinoflagellates1. J. Eukaryot. Microbiol. 58 (3), 203-214.

Harvey, E.L., Menden-Deuer, S., 2011. Avoidance, movement, and mortality: The interactions between a protistan grazer and *Heterosigma akashiwo*, a harmful algal bloom species. Limnol. Oceanogr. 56 (1), 371-378.

Heck, R.H., Tabata, L., Thomas, S.L., 2013. Multilevel and longitudinal modeling with IBM SPSS. Routledge.

Heinbokel, J.F., 1978. Studies on the functional role of tintinnids in the Southern California Bight. I. Grazing and growth rates in laboratory cultures. Mar. Biol. 47, 177-189.

Holen, D.A., Boraas, M.E., 1991. The feeding behavior of *Spumella* sp. as a function of particle size: Implications for bacterial size in pelagic systems. Hydrobiologia 220 (1), 73-88.

Huelsenbeck, J.P., Bollback, J.P., 2001. Empirical and hierarchical Bayesian estimation of ancestral states. Syst. Boil. 50 (3), 351-366.

Huntley, M., Sykes, P., Rohan, S., Marin, V., 1986. Chemically-mediated rejection of dinoflagellate prey by the copepods *Calanus pacificus* and *Paracalanus parvus*: mechanism, occurrence and significance. Mar. Ecol. Prog. Ser. 28 (10).

Jang, S.H., Jeong, H.J., Lim, A.S., Kwon, J.E., Kang, N.S., 2016. Feeding by the newly described heterotrophic dinoflagellate *Aduncodinium glandula*: having the most diverse prey species in the family Pfiesteriaceae. Algae 31 (1), 17-31.

Jeong, H.J., 1994. Predation by the heterotrophic dinoflagellate Protoperidinium cf. divergens on copepod eggs and early naupliar stages. Mar. Ecol. Prog. Ser. 114, 203-203.

Jeong, H.J., 1999. The ecological roles of heterotrophic dinoflagellates in marine planktonic community. J. Eukaryot. Microbiol. 46 (4), 390-396.

Jeong, H.J., Shim, J.H., Lee C.W., Kim J.S., Koh S.M., 1999. Growth and Grazing Rates of the Marine Planktonic Ciliate *Strombidinopsis* sp. on

Red□Tide and Toxic Dinoflagellates. J. Eukaryot. Microbiol. 46 (1), 69-76.

Jeong, H.J., Kim, S.K., Kim, J.S., Kim, S.T., YOO, Y.D., Yoon, J.Y., 2001. Growth and grazing rates of the heterotrophic dinoflagellate *Polykrikos kofoidii* on red□tide and toxic dinoflagellates. J. Eukaryot. Microb. 48 (3), 298-308.

Jeong, H.J., Park, K.H., Kim, J.S., Kang, H.J., Kim, C.H., Choi, H.J., Kim, Y.S., Park, J.Y., Park, M.G., 2003. Reduction in the toxicity of the dinoflagellate *Gymnodinium catenatum* when fed on by the heterotrophic dinoflagellate *Polykrikos kofoidii*. Aquat. Microb. Ecol. 31 (3), 307-312.

Jeong, H.J., Yoo, Y.D., Kim, J.S., Kang, N.S., Kim, T.H., Kim, J.H., 2004. Feeding by the marine planktonic ciliate *Strombidinopsis jeokjo* on common heterotrophic dinoflagellates. Aquat. Microb. Ecol. 36 (2), 181-187.

Jeong, H.J., Song, J.E., Kang, N.S., Kim, S., Yoo, Y.D., Park, J.Y., 2007. Feeding by heterotrophic dinoflagellates on the common marine heterotrophic nanoflagellate *Cafeteria* sp. Mar. Ecol. Prog. Ser. 333, 151-160.

Jeong, H.J., Seong, K.A., YOO, Y.D., Kim, T.H., Kang, N.S., Kim, S., Park, J.Y., Kim, J.S., Kim, G.H., Song, J.Y., 2008. Feeding and grazing impact by small marine heterotrophic dinoflagellates on heterotrophic bacteria. J. Eukaryot. Microb. 55 (4), 271-288.

Jeong, H.J., Yoo, Y.D., Kang, N.S., Rho, J.R., Seong, K.A., Park, J.W., Nam, G.S., Yih, W.H., 2010a. Ecology of *Gymnodinium aureolum*. I. Feeding in western Korean waters. Aquat. Microb. Ecol. 59, 239-255.

Jeong, H.J, Yoo, Y.D., Kim, J.S., Seong, K.A., Kang, N.S., Kim, T.H., 2010b. Growth, feeding, and ecological roles of the mixotrophic and heterotrophic dinoflagellates in marine planktonic food webs. Ocean Sci. J. 45, 65-91.

Jeong, H.J., Lee, K.H., Yoo, Y.D., Kang, N.S., Lee, K.T., 2011. Feeding by the newly described, nematocyst-bearing heterotrophic dinoflagellate *Gyrodiniellum shiwhaense*. J. Eukaryot. Microbiol. 58, 511-524.

Jeong, H.J., Yih, W., Kang, N.S., Lee, S.Y., Yoon, E.Y., Yoo, Y.D., Kim, H.S., Kim, J. H., 2012a. First report of the epiphytic benthic dinoflagellates *Coolia canariensis* and *Coolia malayensis* in the waters off Jeju Island, Korea: morphology and rDNA sequences. J. Eukaryot. Microbiol. 59 (2), 114-133.

Jeong, H.J., Lim, A.S., Jang, S.H., Yih, W.H., Kang, N.S., Lee, S.Y., Yoo, Y.D., Kim, H.S., 2012b. First report of the epiphytic dinoflagellate *Gambierdiscus caribaeus* in the temperate waters off Jeju Island, Korea: morphology and molecular characterization. J. Eukaryot. Microbiol. 59 (6), 637-650.

Jeong, H.J., Yoo, Y.D., Lee, K.H., Kim, T.H., Seong, K.A., Kang, N.S., Lee, S.Y., Kim, J.S., Kim, S., Yih, W.H., 2013. Red tides in Masan Bay, Korea in 2004–2005: I. Daily variations in the abundance of red-tide organisms and environmental factors. Harmful Algae 30, S75-S88.

Jeong, H.J., Lim, A.S., Franks, P.J., Lee, K.H., Kim, J.H., Kang, N.S., Lee, M.J., Jang, S.H., Lee, S.Y., Yoon, E.Y., Park, J.Y., Yoo, Y.D., Seong, K.A., Kwon, J.E., Jang, T.Y., 2015. A hierarchy of conceptual models of red-tide generation: Nutrition, behavior, and biological interactions. Harmful Algae 47, 97-115.

Jeong, H.J., Ok, J.H., Lim, A.S., Kwon, J.E., Kim, S.J., Lee, S.Y., 2016. Mixotrophy in the phototrophic dinoflagellate *Takayama helix* (family Kareniaceae): Predator of diverse toxic and harmful dinoflagellates. Harmful Algae 60, 92-106.

Jeong, H.J., Kim, J.S., Lee, K.H., Seong, K.A., Yoo, Y.D., Kang, N.S., Kim, T.H., Song, J.Y., Kwon, J.E., 2017. Differential interactions between the nematocyst-bearing mixotrophic dinoflagellate *Paragymnodinium*

shiwhaense and common heterotrophic protists and copepods: Killer or prey. Harmful Algae 62, 37-51.

Johnson, M.D., Rome, M., Stoecker, D.K., 2003. Microzooplankton grazing on *Prorocentrum minimum* and *Karlodinium micrum* in Chesapeake Bay. Limnol. Oceanogr. 48, 238-248.

Jürgens, K., Wickham, S.A., Rothhaupt, K.O., Santer, B., 1996. Feeding rates of macro□and microzooplankton on heterotrophic nanoflagellates. Limnol. Oceanogr. 41 (8), 1833-1839.

Kahn, P., Herfort, L., Peterson, T.D., Zuber, P., 2014. Discovery of a *Katablepharis* sp. in the Columbia River estuary that is abundant during the spring and bears a unique large ribosomal subunit sequence element. Microbiol. 3 (5), 764-776.

Kamiyama, T., Matsuyama, Y., 2005. Temporal changes in the ciliate assemblage and consecutive estimates of their grazing effect during the course of a *Heterocapsa circularisquama* bloom. J. Plank. Res. 27 (4), 303-311.

Kamiyama, T., Itakura, S., Nagasaki, K., 2000. Changes in microbial loop components: effects of a harmful algal bloom formation and its decay. Aquat. Microb. Ecol. 21, 21-30.

Kamiyama, T., Suzuki, T., Okumura, Y., 2006. Feeding of the tintinnid ciliate Favella taraikaensis on the toxic dinoflagellate *Alexandrium*

tamarense and the fate of prey toxins. African J. Mar. Sci. 28 (2), 343-346.

Kang, N.S., Jeong, H.J., Yoo, Y.D., Yoon, E.Y., Lee, K.H., Lee, K., Kim, K.H., 2011. Mixotrophy in the newly described phototrophic dinoflagellate *Woloszynskia cincta* from western Korean waters: Feeding mechanism, prey species, and effect of prey concentration. J. Eukaryot. Microbiol. 58 (2), 152-170

Kiefer, D.A., Lasker, R., 1975. Two blooms of *Gymnodinium splendens*, an unarmored dinoflagellate. Fish. Bull. U.S. 73, 675–678.

Kim, J.S., Jeong, H.J., 2004. Feeding by the heterotrophic dinoflagellates *Gyrodinium dominans* and *G. spirale* on the red-tide dinoflagellate *Prorocentrum minimum*. Mar. Ecol. Prog. Ser. 280, 85-94.

Kim, J.S., Jeong, H.J., Yoo, Y.D., Kang, N.S., Kim, S.K., Song, J.Y., Lee, M.J., Kim, S.T., Kang, J.H., Seong, K.A., Yih, W.H., 2013. Red tides in Masan Bay, Korea in 2004-2005: Ⅲ. Daily variation in the abundance of mesozooplankton and their grazing impact on red tide organisms. Harmful Algae 30S, S102-S113.

Kiφrboe, T., Titelman, J., 1998. Feeding, prey selection and prey encounter mechanisms in the heterotrophic dinoflagellate *Noctiluca scintillans*. J. Plank. Res. 20 (8), 1615-1636.

Kühn, S.F., Drebes, G., Schnepf, E., 1996. Five new species of the nanoflagellate *Pirsonia* in the German Bight, North Sea, feeding on planktic diatoms. Helgol. Meeresunters. 50 (2), 205-222.

Laza-Martinez, A., Orive, E., Miguel, I., 2011. Morphological and genetic characterization of benthic dinoflagellates of the genera *Coolia*, *Ostreopsis* and *Prorocentrum* from the south-eastern Bay of Biscay. Eur. J. Phycol. 46 (1), 45-65.

Leaw, C.P., Lim, P.T., Cheng, K.W., Ng, B.K., Usup, G., 2010. Morphology and molecular characterization of a new species of thecate benthic dinoflagellate, *Coolia malayensis* sp. Nov. (dinophyceae). J. Phycol. 46 (1), 162-171.

Lee, S.H., 1993. Measurement of carbon and nitrogen biomass and biovolume from naturally derived marine bacterioplankton. In: Kemp, P.F., Sherr, B.F., Sherr, E.B., Cole, J.J. (Eds.), Aquatic Microbial Ecology. Lewis Publishers, Boca Raton, FL, pp. 319-325.

Lee, S., Fuhrman, J.A., 1987. Relationships between biovolume and biomass of naturally derived marine bacterioplankton. Appl. Environ. Microbiol. 53 (6), 1298-1303.

Lee, R.E., Kugrens, P., 1991. *Katablepharis ovalis*, a colorless flagellate with interesting cytological characteristics. J. Phycol. 27 (4), 505-513.

Lee, K.H., Jeong, H.J., Jang, T.Y., Lim, A.S., Kang, N.S., Kim, J.H., Kim, K.Y., Park, K.T., Lee, K., 2014. Feeding by the newly described mixotrophic dinoflagellate *Gymnodinium smaydae*: Feeding mechanism, prey species, and effect of prey concentration. J. Exp. Mar. Biol. Ecol. 459, 114-125.

Lee, K.H., Jeong, H.J., Kwon, J.E., Kang, H.C., Kim, J.H., Jang, S.H., Park, J.Y., Yoon, E.Y., Kim, J.S., 2016. Mixotrophic ability of the phototrophic dinoflagellates *Alexandrium andersonii*, *A. affine*, and *A. fraterculus*. Harmful Algae 59, 67-81.

Lee, S.Y., Jeong, H.J., Seong, K.A., Lim, A.S., Kim, J.H., Lee, K.H., Lee, M.J., Jang, S.H., 2017. Improved real-time PCR method for quantification of the abundance of all known ribotypes of the ichthyotoxic dinoflagellate *Cochlodinium polykrikoides* by comparing 4 different preparation methods. Harmful Algae 63, 23-31.

Levinsen, H., Nielsen, T.G., 2002. The trophic role of marine pelagic ciliates and heterotrophic dinoflagellates in arctic and temperate coastal ecosystems: A cross□latitude comparison. Limnol. Oceanogr. 47 (2), 427-439.

Lim, A.S., Jeong, H.J., Kim, J.H., Jang, S.H., Lee, M.J., Lee, K., 2015. Mixotrophy in the newly described dinoflagellate *Alexandrium*

pohangense: A specialist for feeding on the fast-swimming ichthyotoxic dinoflagellate *Cochlodinium polykrikoides*. Harmful Algae 49, 10-18.

Lim, A.S., Jeong, H.J., Kim, J.H., Lee, S.Y., 2017. Control of ichthyotoxic *Cochlodinium polykrikoides* using the mixotrophic dinoflagellate *Alexandrium pohangense*: A potential effective sustainable method. Harmful Algae 63, 109-118.

Lim, A.S., Jeong, H.J., Ok, J.H., Kim, S.J., 2018. Feeding by the harmful phototrophic dinoflagellate *Takayama tasmanica* (Family Kareniaceae). Harmful algae 74, 19-29.

Litaker, R.W., Vandersea, M.W., Kibler, S.R., Reece, K.S., Stokes, N.A., Steidinger, K.A., Millie, D.F., Bendis, J., Pigg, R.J., Tester, P.A., 2003. Identification of *Pfiesteria piscicida* (Dinophyceae) and *Pfiesteria*-like organisms using internal transcribed spacer-specific PCR assays. J. Phycol. 39, 754–761.

Matsuoka, K., Cho, H.J., Jacobson, D.M., 2000. Observations of the feeding behavior and growth rates of the heterotrophic dinoflagellate *Polykrikos kofoidii* (Polykrikaceae, Dinophyceae). Phycologia 39 (1), 82-86.

Matsuyama, Y., 1999. Harmful effect of dinoflagellate *Heterocapsa circularisquama* on shellfish aquaculture in Japan. Jap. Agricult. Res. Quart. 33, 283–293.

Matsuyama, Y., Nagai, K., Mizuguchi, T., Fujiwara, M., Ishimura, M., Yamaguchi, M., Uchida, T., Honjo, T., 1995. Ecological features and mass mortality of pearl oysters during the red tide of *Heterocapsa* sp. in Ago Bay in 1992. Nippon Suisan Gakkaishi 61, 35–41.

Medlin, L., Elwood, H.J., Stickel, S., Sogin, M.L., 1988. The characterization of enzymatically amplified eukaryotic 16S-like rRNA-coding regions. Gene 71 (2), 491–499.

Menden-Deuer, S., Lessard, E.J., 2000. Carbon to volume relationships for dinoflagellates, diatoms, and other protist plankton. Limnol. Oceanogr. 45 (3), 569-579.

Mitra, A., Flynn, K.J., Tillmann, U., Raven, J.A., Caron, D., Stoecker, D.K., Wilken, S., 2016. Defining planktonic protist functional groups on mechanisms for energy and nutrient acquisition: incorporation of diverse mixotrophic strategies. Protist 167 (2), 106-120.

Montagnes, D.J.S., Berger, J.D., Taylor, F.J.R., 1996. Growth rate of the marine planktonic ciliate *Strombidinopsis cheshiri* Snyder and Ohman

as a function of food concentration and interclonal variability. J. Exp. Mar. Biol. Ecol. 206 (1-2), 121-132.

Nakamura, Y., Yamazaki, Y., Hiromi, J., 1992. Growth and grazing of a heterotrophic dinoflagellate, *Gyrodinium dominans*, feeding on a red tide flagellate, *Chattonella antiqua*. Mar. Ecol. Prog. Ser. 275-279.

Nakamura, Y., Suzuki, S.Y., Hiromi, J., 1995. Growth and grazing of a naked heterotrophic dinoflagellate, *Gyrodinium dominans*. Aquat. Microb. Ecol. 9 (2), 157-164.

Nakamura, Y., Turner, J.T., 1997. Predation and respiration by the small cyclopoid copepod *Oithona similisr*: How important is feeding on ciliates and heterotrophic flagellates?. J. Plankton Res. 19 (9), 1275-1288.

Norén, F., Moestrup, Ø., Rehnstam-Holm, A.S., 1999. *Parvilucifera infectans* Norén et Moestrup gen. et sp. nov.(Perkinsozoa phylum nov.): a parasitic flagellate capable of killing toxic microalgae. European J. Protistol. 35 (3), 233-254.

Norland, S., 1993. The relationship between biomass and volume of bacteria. In: Kemp, P.F., Sherr, B.F., Sherr, E.B., Cole, J.J. (Eds.), Aquatic Microbial Ecology. Lewis Publishers, Boca Raton, FL, pp. 303-307.

Ohno, H., Endo, Y., Sato-Okoshi, W., Nishitani, G., 2013. Feeding and growth characteristics of a diatom-feeding flagellate isolated from the bottom sediment of Onagawa Bay, Northeastern Japan. Open J. Mar. Sci. 3, 9-14.

Okamoto, N., Inouye, I., 2005. The Katablepharids are a distant sister group of the Cryptophyta: a proposal for Katablepharidophyta divisio nova/Kathablepharida phylum novum based on SSU rDNA and beta-tubulin phylogeny. Protist 156 (2), 163-179.

Oshima, Y., Blackburn, S.I., Hallegraeff, G.M., 1993. Comparative study on paralytic shellfish toxin profiles of the dinoflagellate *Gymnodinium catenatum* from three different countries. Mar. Biol. 116 (3), 471-476.

Park, T.G., Lim, W.A., Park, Y.T., Lee, C.K., Jeong, H.J., 2013. Economic impact, management and mitigation of red tides in Korea. Harmful Algae 30S, S131-S143.

Patterson, D.J., Larsen, J., 1991. General introduction. In: Patterson, D.H., Larsen, J. (Eds.), The biology of free-living heterotrophic flagellates. The systematics association special volume No 45, Clarendon Press, Oxford, pp. 1-5.

Penna, A., Vila, M., Fraga, S., Giacobbe, M.G., Andreoni, F., Riobó, P., Vernesi, C., 2005. Characterization of *Ostreopsis* and *Coolia*

(Dinophyceae) isolates in the Western Mediterranean sea based on morphology, toxicity and Internal Transcribed Spacer 5.8 S rDNA sequences. J. Phycol. 41 (1), 212-225.

Petitpas, C.M., Turner, J.T., Keafer, B.A., McGillicuddy, D.J., Anderson, D.M., 2015. Zooplankton community grazing impact on a toxic bloom of Alexandrium fundyense in the Nauset Marsh system, Cape Cod, Massachusetts, USA. Harmful algae 47, 42-55.

Péquin, B., Mohit, V., Poisot, T., Tremblay, R., Lovejoy, C., 2017. Wind drives microbial eukaryote communities in a temperate closed lagoon. Aquat. Microb. Ecol. 78 (3), 187-200.

Pomroy, A.J., 1989. Scanning electron microscopy of *Heterocapsa minima* sp. nov.(Dinophyceae) and its seasonal distribution in the Celtic Sea. Br. Phycol. J. 24 (2), 131-135.

Porter, K.G., Feig, Y.S., 1980. The use of DAPI for identifying and counting aquatic microflora. Limnol. Oceanogr. 25, 943-948.

Reich, A., Lazensky, R., Faris, J., Fleming, L.E., Kirkpatrick, B., Watkins, S., Ullmann, S., Kohler, K., Hoagland, P., 2015. Assessing the impact of shellfish harvesting area closures on neurotoxic shellfish poisoning (NSP) incidence during red tide (*Karenia brevis*) blooms. Harmful Algae 43, 13-19.

Rivier, A., Brownlee, D.C., Sheldon, R.W., Rassoulzadegan, F., 1985. Growth of microzooplankton: A comparative study of bactivorous zooflagellates and ciliates. Mar. Microb. Food Webs 1, 51-60.

Ronquist, F., Huelsenbeck, J.P., 2003. MrBayes 3: Bayesian phylogenetic inference under mixed models. Bioinformatics 19 (12), 1572-1574.

Salas, R., Tillmann, U., Kavanagh, S., 2014. Morphological and molecular characterization of the small armoured dinoflagellate *Heterocapsa minima* (Peridiniales, Dinophyceae). European J. Phycol. 49 (4), 413-428.

Sanders, R.W., 1991. Mixotrophic protists in marine and freshwater ecosystems. J. protozool. 38 (1), 76-81.

Sanders, R.W., Caron, D.A., Berninger, U.G., 1992. Relationships between bacteria and heterotrophic nanoplankton in marine and fresh waters: an inter-ecosystem comparison. Mar. Ecol. Prog. Ser. 1-14.

Schnepf, E., Schweikert, M., 1997. *Pirsonia*, phagotrophic nanoflagellates incertae sedis, feeding on marine diatoms: attachment, fine structure and taxonomy. Arch. Protistenkd. 147 (3), 361-371.

Scholin, C.A., Herzog, M., Sogin, M., Anderson, D.M., 1994. IDENTIFICATION OF GROUP□AND STRAIN□SPECIFIC GENETIC MARKERS FOR GLOBALLY DISTRIBUTED ALEXANDRIUM (DINOPHYCEAE). II. SEQUENCE ANALYSIS OF

A FRAGMENT OF THE LSU rRNA GENE 1. J. Phycol. 30 (6), 999-1011.

Seong, K.A., Jeong, H.J., Kim, S., Kim, G.H., Kang, J.H., 2006. Bacterivory by co-occurring red-tide algae, heterotrophic nanoflagellates, and ciliates on marine bacteria. Mar. Ecol. Prog. Ser. 322, 85-97.

Sherr, E.B., Sherr, B.F., 1994. Bacterivory and herbivory: key roles of phagotrophic protists in pelagic food webs. Microb. Ecol. 28 (2), 223-235.

Sherr, E.B., Sherr, B.F., 2007. Heterotrophic dinoflagellates: a significant component of microzooplankton biomass and major grazers of diatoms in the sea. Mar. Ecol. Prog. Ser. 352, 187-197.

Sherr, E.B., Sherr, B.F., 2016. Phagotrophic protists: central roles in microbial food webs. In Aquatic Microbial Ecology and Biogeochemistry: A Dual Perspective, pp. 3-12.

Sherr, B.F., Sherr, E.B., Fallon, R.D., 1987. Use of monodispersed, fluorescently labeled bacteria to estimate in situ protozoan bacterivory. Appl. Environ. Microbiol. 53 (5), 958-965.

Shimizu, Y., Alam, M., Oshima, Y., Fallon, W.E., 1975. Presence of four toxins in red tide infested clams and cultured *Gonyaulax tamarensis* cells. Biochem. Biophys. Res. Commun. 66 (2), 731-737.

Stamatakis, A., 2006. RAxML-VI-HPC: maximum likelihood-based phylogenetic analyses with thousands of taxa and mixed models. Bioinformatics 22(21), 2688-2690.

Strom, S.L., Buskey, E.J., 1993. Feeding, growth, and behavior of the thecate heterotrophic dinoflagellate *Oblea rotunda*. Limnol. Oceanogr. 38 (5), 965-977.

Suttle, C.A., Chan, A.M., Taylor, W.D., Harrison, P.J., 1986. Grazing of planktonic diatoms by microflagellates. J. Plankton Res. 8 (2), 393-398.

Sieburth, J.M., 1984. Protozoan bacterivory in pelagic marine waters. In: Hobbie, J.E., Williams, P.J.LeB. (Eds.), Heterotrophic activity in the sea. Plenum Press, New York, NY, pp. 405-444.

Simon, M., Azam, F., 1989. Protein content and protein synthesis rates of planktonic marine bacteria. Mar. Ecol. Prog. Ser. 51, 201-213.

Smayda, T.J., 1997. Harmful algal blooms: their ecophysiology and general relevance to phytoplankton blooms in the sea. Limnol. Oceanogr. 42 (5part2), 1137-1153.

Stoecker, D.K., 1998. Conceptual models of mixotrophy in planktonic protists and some ecological and evolutionary implications. Eur. J. Protistol. 34 (3), 281-290.

Stoecker, D.K., Sanders, N.K., 1985. Differential grazing by Acartia tonsa on a dinoflagellate and a tintinnid. J. Plank. Res. 7 (1), 85-100.

Stoecker, D.K., Davis, L.H., Anderson, D.M., 1984. Fine scale spatial correlations between planktonic ciliates and dinoflagellates. J. Plank. Res. 6 (5), 829-842.

Stoecker, D.K., Hansen, P.J., Caron, D.A., Mitra, A., 2017. Mixotrophy in the marine plankton. Ann. Rev. Mar. Sci. 9, 311-335.

Tamura, K., Dudley, J., Nei, M., Kumar, S., 2007. MEGA4: molecular evolutionary genetics analysis (MEGA) software version 4.0. Mol. Boil. Evol. 24(8), 1596-1599.

Tanaka, T., Fujita, N., Taniguchi, A., 1997. Predator-prey eddy in heterotrophic nanoflagellate-bacteria relationships in a coastal marine environment: a new scheme for predator-prey associations. Aquat. Microb. Ecol. 13 (3), 249-256.

Ten-Hage, L., Turquet, J., Quod, J.P., Couté, A., 2000. *Coolia areolata* sp. nov.(Dinophyceae), a new sand-dwelling dinoflagellate from the southwestern Indian Ocean. Phycologia 39 (5), 377-383.

Throndsen, J.A.H.N., 1973. Motility in some marine nanoplankton flagellates. Norw. J. Zool. 21, 193-200.

Tillmann, U., 2004. Interactions between planktonic microalgae and protozoan grazers. J. Eukaryot. Microb. 51, 156-168.

Turner, J.T., 2006. Harmful algae interactions with marine planktonic grazers. In: Granéli, E., Turner, J.T. (Eds.), Ecology of Harmful Algae. Springer-Verlag, Berlin, pp. 259-270.

Turner, J. T., 2014. Planktonic marine copepods and harmful algae. Harmful Algae 32, 81-93.

Turner, J.T., Tester, P.A., 1997. Toxic marine phytoplankton, zooplankton grazers, and pelagic food webs. Limnol. Oceanogr. 42 (5part2), 1203-1213.

Velo-Suárez, L., Brosnahan, M.L., Anderson, D.M., McGillicuddy Jr, D.J., 2013. A quantitative assessment of the role of the parasite *Amoebophrya* in the termination of *Alexandrium fundyense* blooms within a small coastal embayment. PloS one 8 (12), e81150.

Verity, P.G., 1991. Measurement and simulation of prey uptake by marine planktonic ciliates fed plastidic and aplastidic nanoplankton. Limnol. Oceanogr. 36 (4), 729-750.

Vørs, N., 1992. Ultrastructure and autecology of the marine, heterotrophic flagellate *Leucocryptos marina* (Braarud) Butcher 1967 (Katablepharidaceae/Kathablepharidae), with a discussion of the genera *Leucocryptos* and *Katablepharis*/*Kathablepharis*. Eur. J. Protistol. 28 (4), 369-389.

Wakeman, K.C., Yamaguchi, A., Roy, M.C., Jenke-Kodama, H., 2015. Morphology, phylogeny and novel chemical compounds from *Coolia malayensis* (Dinophyceae) from Okinawa, Japan. Harmful Algae 44, 8-19.

West, B.T., 2009. Analyzing longitudinal data with the linear mixed models procedure in SPSS. Eval Health Prof, 32 (3), 207-228.

West, B.T., Welch, K.B., Galecki, A.T., 2014. Linear mixed models: a practical guide using statistical software. Chapman and Hall/CRC.

White, A.W., 1981. Marine zooplankton can accumulate and retain dinoflagellate toxins and cause fish kills. Limnol. Oceanogr. 26 (1), 103-109.

Yoo, Y.D., Jeong, H.J., Kang, N.S., Song, J.Y., Kim, K.Y., Lee, K.T., Kim, J.H., 2010. Feeding by newly described mixotrophic dinoflagellate *Paragymnodinium shiwhaense*: feeding mechanism, prey species, and effect of prey concentration. J. Eukaryot. Microbiol. 57, 145-15.

Yoo, Y.D., Jeong, H.J., Kim, J.S., Kim, T.H., Kim, J.H., Seong, K.A., Lee, S.H., Kang, N.S., Park, J.W., Park, J., Yih, W., 2013a. Red tides in Masan Bay, Korea in 2004-2005: II. Daily variations in the abundance of heterotrophic protists and their grazing impact on red-tide organisms. Harmful Algae 30S, S89-S101.

Yoo, Y.D., Yoon, E.Y., Jeong, H.J., Lee, K.H., Hwang, Y.J., Seong, K.A., Park, J.Y., 2013b. The newly described heterotrophic dinoflagellate *Gyrodinium moestrupii*, an effective protistan grazer of toxic dinoflagellates. J. Eukaryot. Microbiol. 60 (1), 13-24.

Yoo, Y.D., Jeong, H.J., Lee, S.Y., Yoon, E.Y., Kang, N.S., Lim, A.S., Lee, K.H., Jang, S.H., Park, J.Y., Kim, H.S., 2015. Feeding by heterotrophic protists on the toxic dinoflagellate Ostreopsis cf. ovata. Harmful algae 49, 1-9.

Yoon, E.Y., Kang, N.S., Jeong, H.J., 2012. *Gyrodinium moestrupii* n. sp., a new planktonic heterotrophic dinoflagellate from the coastal waters of western Korea: morphology and ribosomal DNA gene sequence. J. Eukaryot. Microbiol. 59 (6), 571-586.

Zwirglmaier, K., Spence, E.D., Zubkov, M.V., Scanlan, D.J., Mann, N.H., 2009. Differential grazing of two heterotrophic nanoflagellates on marine *Synechococcus* strains. Environ. Microbiol. 11 (7), 1767-1776.

국문 초록

종속영양성 미세조류는 어디에나 있고, 박테리아의 주요 포식자로 알려져 있다. 그러나, 식물성 플랑크톤을 섭식하는 종속영양성 미세조류의 섭식에 대한 이해가 부족하다. 이 두가지 요소들은 일반적으로 공존하는데, 주요 종속영양성 미세조류인 *Katablepharis* 종들의 섭식과 생태학적 역할을 조사하기 위하여 박테리아와 식물성 플랑크톤을 섭식하는 *Katablepharis japonica* 의 섭식 능력과 어떠한 먹이 유형을 먹는지에 대한 조사를 하였다. 더군다나, *K. japonica* 의 성장률과 와편모조류인 *Akashiwo sanguinea*(적절한 조류 먹이), 종속영양성 박테리아, 그리고 남세균인 *Synechococcus* sp.를 먹이로 하였을 때 소화율을 먹이 농도에 따른 함수로 밝혀냈다. 먹이 실험 대상 중에, *K. japonica* 는 종속영양성 박테리아, *Synechococcus* sp., 담녹조강인 *Pyramimonas* sp., 은편모조류인 *Rhodomonas salina* 와 *Teleaulax* sp., 침편모조류인 *Heterosigma akashiwo* 와 *Chattonella ovate,* 와편모조류인 *Heterocapsa rotundata, Amphidinium carterae, Prorocentrum donghaiense*, *Alexandrium minutum*, *Cochlodinium polykrikoides*, *Gymnodinium catenatum*, *A. sanguinea*, *Coolia malayensis*, 그리고 섬모충인 *Mesodinium rubrum* 을 소화했지만, 와편모조류인 *Alexandrium catenella*, *Gambierdiscus*

caribaeus, *Heterocapsa triquetra, Lingulodinium polyedrum*, *Prorocentrum cordatum*, *P. micans, Scrippsiella acuminata* 와 규조류인 *Skeletonema costatum* 는 섭식하지 못하였다. 많은 *K. japonica* 세포들이 함께 공격하며 먹이 세포의 표면을 쪼아서 섭식한 후 파열된 세포 표면에서 나온 물질들을 흡수한다. *A. sanguinea* 는 *K. japonica* 의 양의 성장을 지지했지만, 종속영양성 박테리아와 *Synechococcus* sp.는 성장을 지지하지 못하였다. *A. sanguinea* 를 섭식한 *K. japonica* 의 최대 특정 성장률은 1.01 d^{-1} 이고, 최대 소화율은 0.13 ng C $predator^{-1}d^{-1}$ (0.06 cells $predator^{-1}d^{-1}$) 이다. 종속영양성 박테리아를 섭식한 *K. japonica* 의 최대 소화율은 0.019 ng C $predator^{-1}d^{-1}$ (226 bacteria $predator^{-1}d^{-1}$) 이고, *Synechococcus* sp.를 섭식한 *K. japonica* 의 가장 높은 소화율은 (약 10^7 cells ml^{-1} 의 농도로 먹이 제공) 0.01 ng C $predator^{-1}d^{-1}$ (48 *Synechococcus* $predator^{-1}d^{-1}$) 이다. *A. sanguinea*, 종속영양성 박테리아, *Synechococcus* sp.로부터의 최대 일일 탄소 유입량은 포식자의 몸 탄소의 각각 307, 43, 22%였다. 따라서, 종속영양성 박테리아와 *Synechococcus* sp.를 섭식한 *K. japonica* 의 낮은 소화율은 성장 부족의 원인이 될 수 있다. 이 연구의 결과는, *K. japonica* 는 유독하거나 해로운 조류를 포함한 다양한 식물성 플랑크톤의 포식자이며, 먹이 종들에 의해

야기되는 적조의 역학에도 영향을 미칠 수 있다는 것을 분명히 보여 준다.

이 연구 이전에, 광합성 와편모조류인 *Heterocapsa minima* 는 한국 해역에서 보고되지 않았었다. 나는 2016 년에 한국 미조항에서 이 종을 분리하였다. *Heterocapsa* 속은 주요 적조나 유해한 와편모조류 중 하나로 기록되어 있다. *H. minima* 의 효과적인 포식자를 조사하기 위하여, engulfment-feeding 을 하는 종속영양성 와편모조류인 *Oxyrrhis marina*, *Gyrodinium dominans*, *Polykrikos kofoidii* 와 peduncle-feeding 을 하는 종속영양성 와편모조류인 *Pfiesteria piscicida,* pallium-feeding 을 하는 종속영양성 와편모조류인 *Oblea rotunda*, 무갑섬 섬모충 *Pelagostrobilidium* sp.에 *H. minima* 를 먹이로 제공하여 실험하였다. 나는 *O. marina*, *G. dominans*, *P. piscicida*, *Pelagostrobilidium* sp.가 *H. minima* 를 섭식 가능한 것을 발견하였다. 그러나, *H. minima* 는 포식자들의 성장에 영향을 미치지 않았다. 이러한 연구 결과들은, 종속영양성 포식자들이 *H. minima* 에 끼치는 포식의 영향이 무시할 수 있을 것이라는 것을 암시한다.

Keywords: 와편모조류, 원생생물, 섭식, 성장, 소화, 유해적조, 적조

Student Number: 2016-20404